Exploring the therapeutic potential of a peptide derived from a poxviral immune evasion protein

Dylan Lawless

A thesis submitted to the School of Biochemistry and Immunology

Trinity College Dublin

The University of Dublin

In partial fulfilment of the requirements for degree of

Master of Science

Immunology

June 2014

Table of Contents

Abstract

1. Introduction

1.1 Toll-like receptors detect bacterial and viral ligands

1.2 TLR TIR domain interactions

1.3 Adaptor protein signal transduction

1.4 Crystal structure of the Mal TIR domain

1.5 TLR4 TIR domain Interacts with TRAM and Mal

1.6 Mal and TRAM involvement with TLR4 TIR domain occurs sequentially

1.7 TLR2 ligands can induce type I IFN responses

1.8 VACV A46 targets specific TIR-domain-containing adaptors

1.9 Other poxviral immune evasion mechanisms

1.10 A46 Bcl-2 fold targets the BB loop of TLR TIR domains

1.11 VIPER: Inhibitory peptide derived from A46

1.12 Nuclear magnetic resonance spectroscopy

1.13 Final summary

2. Materials and Methods

2.1 Materials

2.1.1 Cell culture

2.1.2 Antibodies

2.1.3 Receptor agonists

2.2 Methods

2.2.1 Cell culture

2.2.2 Peptide synthesis and reconstitution

2.2.3 Enzyme-Linked ImmunoSorbent Assay (ELISA)

2.2.4 MTT assay

2.2.5 Statistical analysis

2.3 NMR analysis

2.3.1 NMR Experiments

2.3.2 Pulse sequence details for MNR data acquisition

2.3.3. NMR peak assignment

3. Results

3.1. TLR4 inhibition

3.1.1 9R-VIPER has greater inhibitory properties than VIPER for LPS driven TNFα in both wt iBMDM and human PBMC

3.1.2 9R-VIPER has greater inhibitory properties than VIPER for LPS driven IFNβ in wt iBMDM

3.1.3 9R-VIPER and VIPER inhibit for LPS driven IP-10 equally well in PBMC

3.2 TLR2 inhibition

3.2.1 VIPER and 9R-VIPER reduce TLR2-driven TNFα in wt iBMDM and PBMC

3.2.2 9R-VIPER has greater inhibitory properties than VIPER for Malp-2 driven IFNβ in both wt iBMDM and human PBMC

3.3 9R-VIPER peptide residues required for effective TLR4 signal inhibition in wt iBMDM and human PBMC

3.4 Longevity of TLR4 inhibition by VIPER and 9R-VIPERin wt iBMDM and human PBMC

3.5 NMR determination of peptide structure

3.5.1 9R-VIPER structure

3.5.2 9R-VIPER mutant L6AE10A structure

4. Discussion

5. Conclusion

7. References

8. Abbreviations

List of Figures List of Tables

Figure 1.1 Signalling adaptors involved in TLR4 and TLR2 activation of pro-inflammatory and interferon related genes

Figure 1.2 Interactions of TLR4 TIR domains and their signalling adaptors after endocytosis of activated TLR4 viewed from above

Figure 1.3 Mal and TRAM interactions with TLR4 TIR domain

Table 2.1. Peptide Sequences

Table 2.2 ELISA capture and detection antibody dilution factor

Figure

3.1. TLR4 inhibition

3.1.1 Inhibitory properties of 9R-VIPER and VIPER for LPS driven TNFα in wt iBMDM

3.1.2 Affect on cell viability determined by MTT

3.1.3 Inhibitory properties of 9R-VIPER and VIPER for LPS driven TNFα in human PBMC

3.1.4 Inhibitory properties of 20uM 9R-VIPER and VIPER for LPS driven TNFα in human PBMC

3.1.5 Inhibitory properties of 9R-VIPER and VIPER for LPS driven IFNβ in wt iBMDM and LPS driven IP-10 in PBMC

3.1.6 Inhibitory properties of 5 μM 9R-VIPER and VIPER in human PBMC (Supplemental)

3.2 TLR2 inhibition

3.2.1 Inhibitory properties of 9R-VIPER and VIPER for Malp-2 driven TNFα in wt iBMDM and human PBMC

3.2.2 Inhibitory properties of 9R-VIPER and VIPER for Malp-2 driven IFNβ in wt iBMDM and Malp-2 driven IP-10 in PBMC

3.2.3 Inhibitory properties of 5 μM 9R-VIPER and VIPER for Malp-2 IP-10 in PBMC (Supplemental)

3.3 Mutant peptides activity

3.3.1 9R-VIPER peptide residues required for effective TLR4 signal inhibition in wt iBMDM and human PBMC

3.3.2 9R-VIPER peptide residues required for effective TLR2 signal inhibition in wt iBMDM and human PBMC (Supplemental)

3.4 Longevity of TLR4 signal inhibition

3.4.1 Longevity of TLR4 inhibition by VIPER and 9R-VIPER prior to stimulation

3.4.2 Longevity of TLR4 inhibition by VIPER and 9R-VIPER after stimulation

3.5 NMR structure

3.5.1 Cartoon representation of the 9R-VIPER 3D structure based on NRM data

3.5.2 2D structure of VIPER and 9R-VIPER sequence

3.5.3 HN-HSQC of VIPER and 9R-VIPER

3.5.4 9R-VIPER NOESY spectrum

3.5.5 9R-VIPER TOCSY spectrum

3.5.6 TOCSY/NOESY spectra sections from Mutant peptide

Abstract

Toll-like receptors (TLRs) have a role in viral detection leading to cytokine and IFN induction, and as such are targeted by viruses for immune evasion. The poxviral protein A46 has been identified to inhibit TLR signalling by interacting with Toll-IL-1 receptor (TIR) domain containing proteins of the receptor complex to collectively inhibit all TLR adaptor proteins that positively regulate transcription-factor activation. An inhibitory peptide derived from A46 termed VIPER selectively targets TLR4. This research investigates what affect the polyarginine delivery sequence location has on VIPER activity in vitro. 9R-VIPER is shown to be more effective at TLR4 and TLR2 signal inhibition than VIPER for multiple signalling pathways. Novel mechanisms of TLR2-driven interferon induction have been shown to be affected by 9R-VIPER and VIPER. The longevity of TLR4 inhibition by 9R-VIPER was shown to be superior to VIPER. Residues required for peptide activity were identified. Structural information about 9R-VIPER and a loss-of-function mutant was determined by NMR analysis. The results presented here provide insights into the mechanics of TLR4 and TL2 signalling pathways and explores the therapeutic potential of the VIPER peptide derived from a poxviral immune evasion protein.

1. Introduction

Viruses are obligate parasites that rely on host proteins for their own life cycle and require strategies to evade and modulate the immune response. Viral infection leads to the initiation of antiviral innate immune responses, inducing the expression of the type I interferons (IFNs) IFNα and IFNβ, and pro-inflammatory cytokines. Type I IFNs also regulate the adaptive immune response by priming T helper cells and cytotoxic T cells. Numerous viral mechanisms have been identified which modulate the pathogen detection response to

promote their own survival. Vaccinia virus (VACV), a member of the poxvirus family and the active constituent of the vaccine that eradicated smallpox, is one such virus which has provided a vast collection of viral inhibitors of the host immune response. Some of the most well defined viral inhibitors target the innate immune signalling mechanisms of pattern recognition receptors (PRRs). Toll-like receptors (TLRs) are a class of surface and endosomal PRR proteins that play a key role in the innate immune system by responding to pathogen-associated molecular patterns (PAMPs). Each set of TLRs responds to particular pathogen components and initiates the production of pro-inflammatory cytokines and chemokines. Signal transduction by TLRs requires the interaction of particular signalling adaptors such as myeloid differentiation primary-response gene 88 (MyD88) and TIR domain-containing adapter inducing IFN-β (TRIF). These signal transduction mechanisms act as host targets of viral inhibition mechanisms, thereby preventing a robust anti-viral immune response. Investigation of the mechanisms required to modulate host signalling pathways can reveal deeper insights into the innate immune response as well as possibly offering therapeutic opportunities for TLR mediated conditions such as sepsis and sterile inflammation. In this Review, I describe recent advances and emerging themes in our understanding of how TLR4 structurally interacts with adaptor proteins and their inhibition by VACV A46 and VIPER.

1.1 Toll-like receptors detect bacterial and viral ligands

TLRs function as dimers to respond to bacterial and viral PAMPs by recruiting adapter proteins. TLRs and their adaptors are members of the Toll/IL-1R (TIR) domain-containing family of proteins. TLR2 heterodimerises with either TLR1 or TLR6 to senses bacterial triacylated lipopeptides or bacterial diacylated lipopeptides respectively. Many TLRs homodimerise, such as TLR3 which detects viral double-stranded RNA, and TLR4 which

responds to gram-negative bacterial lipopolysaccharide. Homodimerisation also occurs with TLR5 which detects bacterial flagellin and TLR9 which detects bacterial and viral unmethylated CpG-containing DNA. TLR8, like TLR7, can sense viral single-stranded RNA by dimerising with TLR7 and TLR9. TLR dimers are believed to occur as pre-formed complexes which undergo conformational change upon ligand binding. This structural change allows for the cytosolic TIR domains of each receptor to come into close proximity and build a signalling platform for adaptor proteins. In each case the resulting signalling complex will allow for activation of transcription factors required for a robust immune response.

1.2 TLR TIR domain interactions

TIR domain interactions mediate homo- and heterodimerisation and enable the formation of signalling complexes [1-3]. TIR domains typically consists of a central five-stranded parallel β-sheet (designated as βA– βE) surrounded by five α -helices (αA– αE) (Figure 1. C). The shared characteristics of different TIR domains allows for interaction of topologically diverse structural regions [4-7]. TLR4 homodimerisation occurs through TIR domain BB loop interaction with E helix [7, 8], whereas TLR1 and TLR2 form a heterodimer by interaction of TLR1 BB loop and TLR2 DD loop [9]. Once dimerised, the cytosolic TIR domains of TLRs are available for adaptor protein binding.

1.3 Adaptor protein signal transduction

Adaptor proteins are differentially used by receptor complexes to positively regulate transcription-factor activation. Of the 13 mammalian TLRs reported to date four adaptors are used for signal transduction: myeloid differentiation primary-response gene 88 (MyD88) [10], a cytoplasmic TIR-domain-containing adaptor known as MyD88-adapter-like (MAL)

[11, 12], TIR domain-containing adapter inducing IFN-β (TRIF) [13], and TRIF-related adapter molecule (TRAM) [14]. A fifth adaptor, known as sterile α and HEAT-armadillo motifs protein (SARM), negatively regulates TRIF-dependent signalling [15].

TLR5, TLR7, TLR8, and TLR9 use the signal adaptor protein MyD88. TLR3 depends on TRIF for signal transduction. The heterodimers of TLR2/1 and TLR2/6 utilise both the adaptors MyD88 and Mal for functional signalling. TLR4 is unique in that two different responses can occur from ligand binding. Four adaptor proteins are utilised for these two different signalling pathways: MyD88 –Mal and TRIF –TRAM. Medzhitov et al. propose that TLR4 engages these two signal transducers at distinct cellular locations sequentially [16] (described later in detail) (Fig.1A). This indicates that the docking site of the TLR4 TIR domain may be sufficient to host several adaptors. It is also possible that Mal and TRAM compete for the same binding site for recruitment to activated TLR4 [4-7]. More recently the structural regions of Mal and TRAM which mediate interaction with TLR4 have become clearer although different models are proposed which disagree on the physical mechanics and timing of interaction. Transcription factor activation occurs through TIR-domain-containing adaptors allowing NFκB, p38, JNK, and IRFs to initiate pro-inflammatory gene expression.

1.4 Crystal structure of the Mal TIR domain

Rather than the BB loop segment present in other TIR domains, the Mal TIR instead contains a long AB loop connecting the first helix A to the B-strand [17, 18]. This structure differs from most TIR domains which normally have a helical B segment between the B- and C-strands. The structural rearrangement present in Mal TIR retains significant sequence similarity to other TIR domains implying that BB loop functional activity is retained by the AB loop. The poxviral protein A46 is dependent on BB type loop to bind to adaptor proteins

as well as being capable of binding Mal [19]. The idea that the Mal AB loop is very similar to other TIR BB loops explains the finding that A46 binds Mal without the requirement of a BB loop. Studies by Valkov et al. [17] suggests that the interacting surface between Mal and TLR4 requires the Mal AB loop. This region is not required for the Mal: Mal nor Mal:MyD88 interaction surface and consequently A46 fails to inhibit Mal:Mal or Mal:MyD88 interactions.

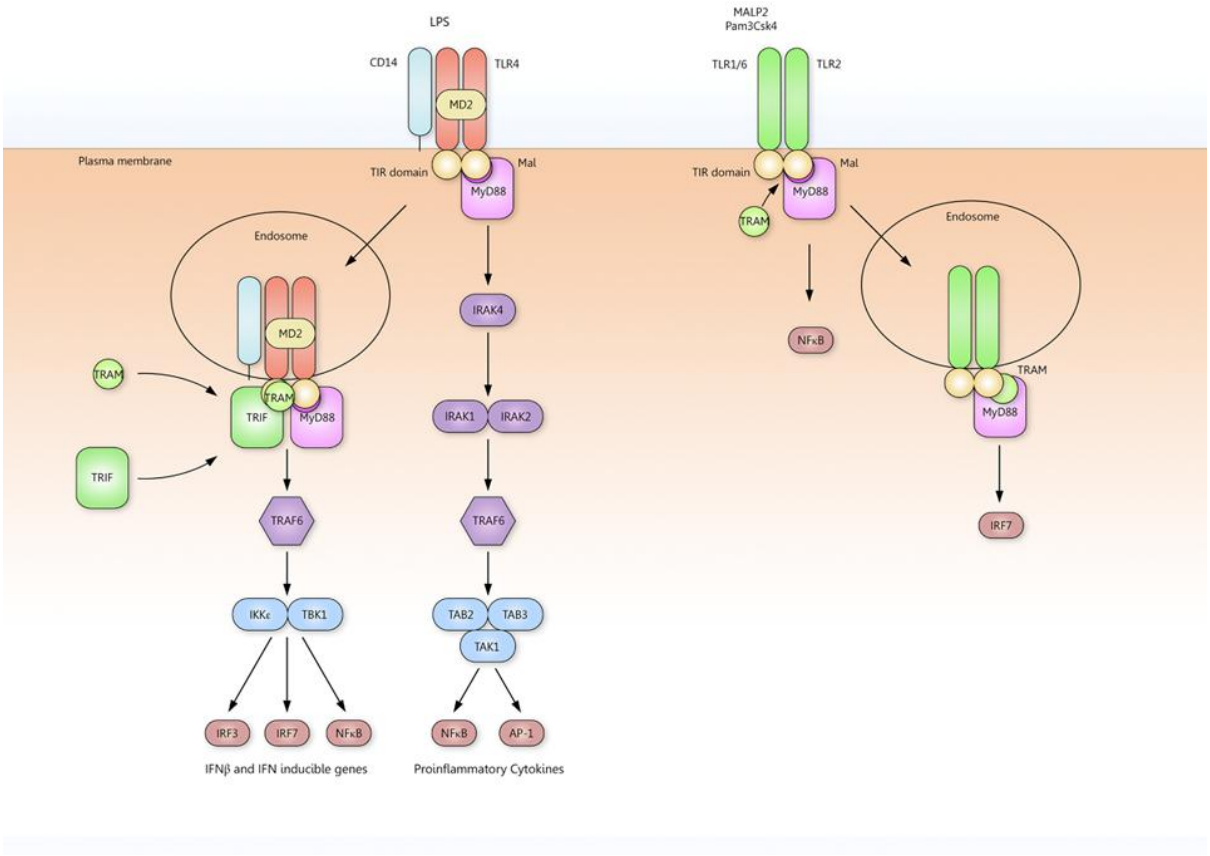

Figure 1.1

Signalling adaptors involved in TLR4 and TLR2 activation of pro-inflammatory and interferon related genes. Mal (shown in dark pink) recruits MyD88 to the plasma membrane, promoting interaction with the cytosolic region of TLR4. Three discrete sites of the MyD88 TIR domain are important for TLR4 signalling, two of which mediate direct binding to the Mal TIR domain. TRAM is thought to be endocytosed along with the TLR4 complex after Mal-dependent signalling. Both MyD88-dependent and TRIF-dependent pathways use TRAF6 to activate the TAB/TAK complex for production of proinflammatory cytokines or the TBK1/IKK complex for production of IFNβ and IFN inducible genes.

TLR2 TIR domain is bound by Mal at the plasma membrane and thereby recruits MyD88 for induction of pro-inflammatory genes. TRAM is believed to be recruited after endocytosis of the TLR2 receptor complex. Here it acts as the signal transducer for interferon related genes.

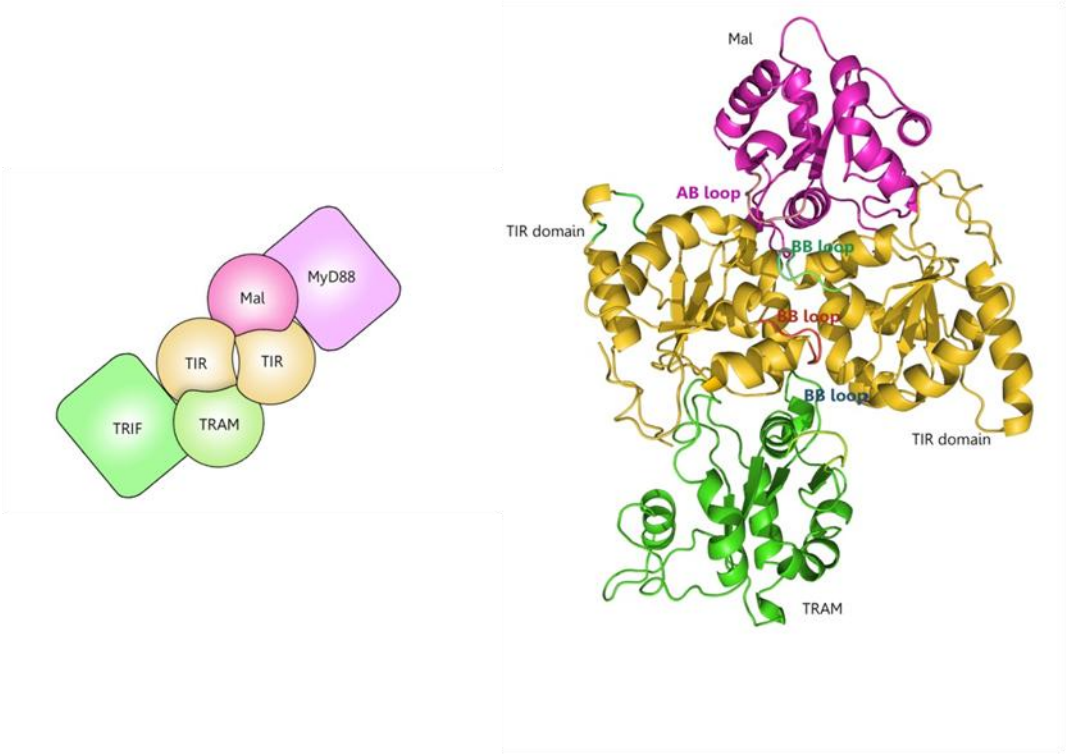

Figure 1.2 Interactions of TLR4 TIR domains and their signalling adaptors after endocytosis of activated TLR4 viewed from above. Pictured on the right is the ribbon loop structures of TLR4 TIR domains and their signalling adaptors viewed from above. The Mal TIR contains a long AB connecting the first helix A to the B-strand. Three discrete sites of the MyD88 TIR domain are important for TLR4 signalling, two of which mediate direct binding to the Mal TIR domain. TRAM uses its TIR BB loop and the third helical region of TIR to dock with the TLR4 TIR domain. TRIF TIR domain associates with TRAM through the TRIF B helix region but uses a different region for TRIF-TLR4 association. The TIR domains of TLR4 dimer interact with each other using their BB loops. Molecular model of MAL and TRAM TIR domains bridged to the activated TLR4 TIR domains adapted from Manavalan et al [20]. MyD88: Myeloid differentiation primary-response gene 88; Mal: MyD88-adapter-like; TRIF: TIR domain-containing adapter inducing IFN-β; TRAM: TRIF-related adapter molecule.

1.5 TLR4 TIR domain Interacts with TRAM and Mal

Of the MyD88-dependent pathways only TLR2 and TLR4 generally require the adaptor protein Mal for efficient signal transduction (TLR2-Mal dependency is discussed later). Kagan and Medzhitov have shown that MyD88 and Mal serve different roles in TLR4 signalling [21]. MyD88 severs as an essential signal adaptor for signal transduction from activated TLR. Mal has been termed to function as a "sorting adaptor" which recruits MyD88 to the plasma membrane, promoting interaction with the cytosolic region of TLR4. TRAM has also been implicated as a "sorting adaptor" [22]. The solution structure of MyD88 has been described using NMR spectroscopy [23]. Three discrete sites of the MyD88 TIR domain are important for TLR4 signalling, two of which mediate direct binding to the Mal TIR domain.

The amino-terminal localisation domain of Mal allows for interaction with phosphatidylinositol-4,5 bisphosphate of the plasma membrane [21]. Here, the TLR4/Mal/MyD88 complex is formed for MyD88-dependent signalling via IL-1R-associated kinases (IRAKs) and TNFR associated factor 6 (TRAF6). Signalling by this pathway results in activation of the transcription factors, AP-1 and NFκB.

TRAM is myristoylated at its amino terminus [24] and has a polybasic domain [16] which are both required for TRAM plasma membrane targeting. However, the myristoylation sequence is also required for endosomal localisation [22]. In this way, the TLR4/TRAM/TRIF complex forms at the endosomal membrane. Activation of the transcription factor IFN regulatory factor 3 (IRF3) occurs via TRAF3 signalling from endocytosed TLR4 [16]. TLR4 signaling causes Mal-dependent NFκB activation for induction of pro-inflammatory genes including TNFα. Conversely, TRAM-dependent IRF3 activation is responsible for TLR4 mediated

IFNβ (Figure 1.1). Recently, Verstak et al. have described the TRAM interaction with TRAF6 contributing to TLR4 mediated inflammatory responses [25].

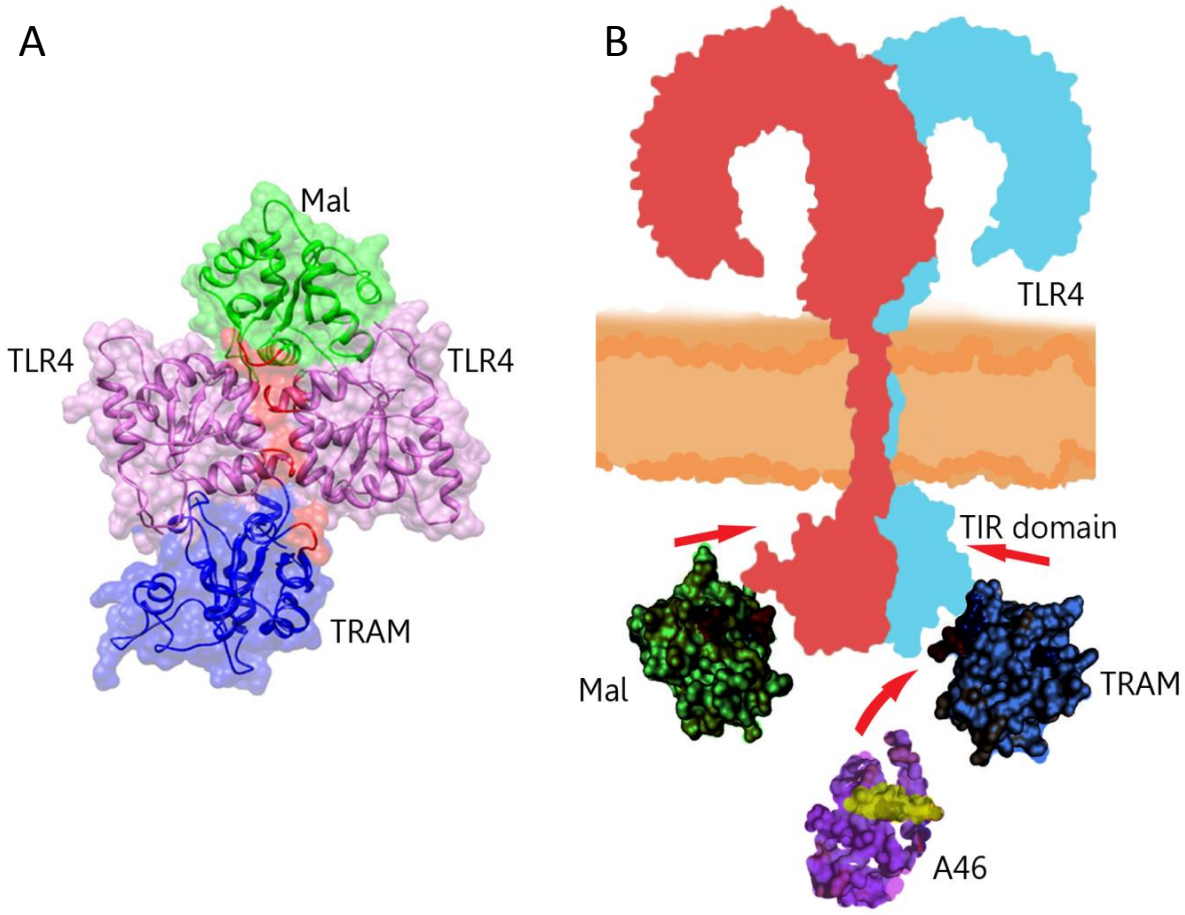

Figure 1.3 Mal and TRAM interactions with TLR4 TIR domain

A. Molecular model of Mal and TRAM TIR domains bridged to the activated TLR4 TIR domains. Mal and TRAM proteins are both predicted to bind to the TLR4 homodimer interface. It is probable that binding of Mal or TRAM protein is mutually exclusive, with the former binding to activated receptors at the cell surface and the latter in endosomes (adapted from Manavalan et al) [20]. **B.** Mal and TRAM interact with the TLR4 TIR domain. A46 is shown to inhibit TRAM. VIPER is shown as yellow on the surface of A46 and is thought to retain its function as an 11 aa peptide. Interpretation of Mal crystal structure [17, 23] and hypothetical representation of TRAM and A46 binding.

1.6 Mal and TRAM involvement with TLR4 TIR domain occurs sequentially

TRAM is thought to be endocytosed along with the TLR4 complex after Mal-dependent signalling [26]. Following endocytosis, conformational change of the receptor believed to facilitating the interaction of TRAM as an adaptor protein. MAPPIT and FLAG-tagging studies by Bovijn et al. indicate that Mal and TRAM both require the same or at least adjacent overlapping binding sites on the TLR4 TIR domain [27] in contrast to the model described earlier [16]. Slightly stronger affinity of Mal than TRAM for the TLR4 TIR domain was shown in this study, which supports the idea that TRAM interacts later than Mal in the endosome. The model proposed here designates three TLR4 TIR binding sites involved in TIR-TIR dimerisation and adaptor interaction. The first site is used for TLR4-TLR4 TIR-TIR interaction. After dimerisation two other identical sites become available which form an extended binding platform providing binding for both Mal and TRAM. This model is based on the inferred form of TLR4 TIR domain using the dimeric TLR10 TIR domain crystal structure. Future studies may still identify subtle differences for this inferred TLR4 TIR-adaptor protein interaction (Figure 1.3).

A similar model has been presented by Nunezl et al. [4] based on in silico docking but different binding sites were predicted for Mal and TRAM. However, the binding sites provided do not have a high amount of conservation and mutations to these sites does not significantly affect adaptor binding or signalling as shown by Ronni et al [28]. Therefore the model of adjacent Mal and TRAM binding sites proposed by Bovijn et al. is more in line with experimental data.

Recently Piao et al. derived peptides from TRAM TIR BB loop and C helix which prevent LPS-induced recruitment of MyD88 to TLR4 as well as co-immunoprecipitation of TRAM

and TLR4 [29]. These studies demonstrate that TRAM uses TIR BB loop and the third helical region of TIR to dock with The TLR4 TIR domain. The decoy peptides blocked these interactions to prevent LPS-induced activation of MyD88-dependent and TRIF-dependent cytokines, as well as MAPK activation. The same group also derived peptides from the TRIF TIR BB loop and putative helix B [30]. Again LPS-induced cytokines and MAPK activation were strongly inhibited by this peptide. Immunoprecipitation assays suggest that the folded TRIF TIR domain associates with TRAM through the TRIF B helix region, but uses a different region for TRIF-TLR4 association. This work identifies TRIF sites that are important for interaction with TLR4 and TRAM (Figure 1.3).

1.7 TLR2 stimulation can induce type I IFN responses

Previously it was believed that TLR3 and TLR4 have evolutionarily diverged from other TLRs in their IRF3 activity towards innate antiviral responses [31]. Until recently, the literature has reported no direct role for TLR2/TLR1 or TLR2/TLR6 heterodimers in type I IFN responses [16, 32]. Hoshino et al. report that TLR2 is not responsible for induced up-regulation of IFN-inducible genes including IP-10. However, section 2. B. of the studies presented here support the current literature of TLR2 induction of IFNβ [33].

An important concept from the work of Kagan et al. showed that for TLRs induced IFNβ at the plasma membrane a shuttling sequence must be provided (in this case, a pleckstrin homology domain of phospholipase C-δ1) at the amino terminus of TRAF3 to allow it to reach TLR2 at the internal cell surface [16].

The explanation for TLR2 induced IFNβ overcoming this subcellular separation of receptor and downstream components is presented to a great extent by Dietrich and colleagues [34].

Sections 1.5 and 1.6 describe the sequential involvement of Mal and TRAM in TLR4 signalling and the different responses arising from distinct sub-cellular sites. Similar to TLR4 activity, TLR2 ligand activation results in receptor internalisation to endolysosomal compartments and the induction of IFN-β via MyD88 and IRF7 [34]. Furthermore, disruption of receptor internalisation or endosome maturation inhibited IFN-β induction yet did not affect NFκB-dependent proinflammatory cytokines like TNF-α. This indicates that both TLR4 and TLR2 share the mechanism of pro-inflammatory and type I IFN responses originating from specific sub-cellular locations, at the plasma membrane and endolysosomal compartments.

More recently, viral nucleic acid have been shown to cause endosome-mediated induction of type I IFNs in several TLRs [35], while gram-positive bacteria are detected by TLR2 recognition of surface components, such as lipoproteins and lipoteichoic acids [36]. Pam3Csk4 is used experimentally as an agonist of the TLR2/TLR1 heterodimer, the ligands responsible for detection of triacylated lipopeptides [37]. Similarly, Malp-2 is used to stimulate TLR2/TLR6 heterodimers which generally sense the fatty acid groups of diacylated lipopeptides and LTA [38, 39]. Vacinia virus is also shown to induce a TLR2-dependent IFNβ response [40]. Viral inhibition of TLR2 may promote VACV immune evasion by abrogating a successful innate response to infection [40].

As mentioned previously, TLR2 also uses Mal as a signalling adaptor for signal transduction via MyD88. However, this dependency for Mal signal transduction is found alter by high levels of ligand stimulation [41]. Furthermore, some downstream TLR2 signalling may be entirely independent of Mal since TLR2/1-mediated Akt phosphorylation can occur in the absence of Mal and MyD88 [42].

Apart from the mechanisms described here, the TLR2 dependent type I IFN signalling pathway is not particularly clear. The adaptor requirements for TLR2-stimulated IFNβ induction is yet to be characterised. Roles for adaptor proteins besides MyD88 have not yet been described.

1.8 VACV A46 targets specific TIR-domain-containing adaptors

Many viruses are capable of interfering with innate signalling pathways through complex intracellular events [43]. These mechanisms can function to inhibit host signalling to prevent viral detection and in some cases promote inflammatory responses to facilitate viral dissemination. Multiple viral antagonists of TLR signalling have been characterised. VACV is a large dsDNA virus of the Poxviridae family. Many of its encoded proteins are secreted from infected cells to inhibit the action of complement factors, interferons, cytokines, and chemokines. Other VACV proteins operate intracellularly to inhibit innate immune signalling pathways [44, 45]. VACV protein A46 was one of the earliest characterised viral inhibitors of TLR signalling [46, 47].

A46 directly targets specific TIR-domain-containing adaptors. Like TLRs and their adaptors, A46 contains a TIR domain and it itself was originally identified on the basis of sequence similarity to TIR domains. This allows it to interact with other TIR-domain-containing complexes to directly bind TLR adaptors; MyD88, Mal, TRIF, and TRAM. Therefore, A46 suppresses multiple TLR pathways preventing activation of NFκB and IRFs [46]. Stack et al. show that deletion of the gene encoding A46R causes attenuation of VACV. Several TLRs participate in the innate immune response to poxvirus infection. Investigations of viral

immune evasion strategies can contribute the understanding of the molecular mechanisms required for pathogen detection.

A critical balance exists between effective and excessive innate immune responses during poxvirus infection. Hutchens et al. [48] report that mice lacking TLR3 had decreased viral replication following vaccinia infection. This indicates that TLR3 increases disease morbidity and mortality during infection. The same group later found that inhibition of TLR4 signaling increased viral replication, hypothermia, and mortality [49]. TLR4 mediates a protective innate immune response against vaccinia which the virus targets with VACV A46 [19]. TLR3 is dependent on the TRIF adaptor protein whereas TLR4 can signal with both TRIF and MyD88. The fifth adaptor protein, SARM, functions as the negative regulator TRIF-dependent signalling further downstream [15]. A46 is capable of inhibiting the TLR4 signalling of both MyD88-dependent and TRIF-dependent pathways. This indicates that A46 antagonises MyD88-dependent signalling at the plasma membrane by inhibiting Mal interaction as well as antagonising TRIF-dependent signalling at the endosome by preventing TRAM function.

1.9 Other poxviral immune evasion mechanisms

A52 is another VACV protein that targets specific signal pathways. It targets TRAF6 and IL-1R-associated kinase 2 (IRAK2), causing inhibition of NFκB activation [50, 51]. Unlike A46, A52 had no effect on TLR-induced IRF activation indicating that IRAK2 does not play a role in TLR activation of IRFs. IRAK2 contributes to different signalling pathways for the activation of NFκB, whereas IRAK1 has a crucial role in the TLR-IRF signalling pathway [43, 52]. Both A46 and A52 contain a bcl-2 fold, which inhibit PRR signalling [52]. Other members of the family of poxviral proteins either demonstrated or predicted to contain a bcl-

2 fold include B14, K7, and C6, which also provide immune evasion mechanisms. All of these proteins share a similar bcl-2-like fold yet interact with a diverse range and structurally different host proteins. VACV B14 and K7 inhibit downstream signalling components [53, 54].

Human DEAD-box protein 3 (DDX3) is targeted by K7 to inhibit PRR-induced activation of IRFs and disrupting the IRF-activating complex that contains TANK-binding kinase 1 (TBK1) and inhibitor of NFκB kinase-ε (IKKε) [55]. C6 binds to TBK-1 adaptor proteins and inhibits activation of IRF3 and IRF7 [56]. C6L is a required virulence factor for VACV, although K7 targets the same complex as C6. This demonstrates the necessity for multiple host immune evasion mechanisms for virus survival.

1.10 A46 Bcl-2 fold targets the BB loop of TLR TIR domains

The crystal structures of A52 and B14 been demonstrated to share a bcl-2-like fold which ultimately inhibits NFκB activation [52]. Biochemical and biophysical analysis have shown the C-terminal region of A46 to bind the TIR domain of Mal [57]. This region of A46 (residues 81 - 230) is characteristic of a Bcl-2 fold due to its highly α-helical structure. A46 may target TIR proteins in a manner not involving homotypic TIR-TIR interactions but using its Bcl-2-like C-terminal region [58]. Other interactions between Bcl-2-like proteins and TIR-containing domains have been identified previously such as the MyD88 and TRIF interaction with Beclin 1 to trigger autophagy in macrophages [59].

Stack et al. have shown that the BB loop proline in TIR proteins is essential for interaction with A46 [19]. TLRs or TIR adaptors lacking this conserved proline cannot be bound by A46. It was also shown here that A46 inhibits TLR4 signalling by disrupting both the TLR4-

MAL and TLR4-TRAM interactions. These receptor:adaptor interactions were shown to be targeted by VACV in vitro. A46 disrupts only receptor:adaptor interaction but not receptor:receptor nor adaptor:adaptor interactions in TLR4. Likewise, TIR BB loop prolines are important in the receptor:adaptor interactions, as required by Mal and TRAM in the interaction with TLR4 [2, 12]. A conserved cysteine is also required for TRAM:TLR4 interaction but not Mal:TLR4 [11, 57].

The dimeric α-helical sub-domain of A46 targets the Mal TIR domain. However, the C-terminal Bcl-2 fold may not be providing the full physical interaction as CD spectroscopy indicates that Mal may also contain 18% β-strand in this region [57].

1.11 VIPER: Inhibitory peptide derived from A46

The use of cell-permeable peptides representing TIR domain BB loops capable of inhibiting TLR signalling lead to the idea of designing inhibitory peptides derived from A46. Viral proteins which have been refined by natural selection for targeting host proteins may be identified and characterised. The viral evasion mechanisms that are required to abate antiviral immune responses have similar results as those provided by anti-inflammatory therapeutics. Therefore, these types of viral peptides can be improved by rational design for use as therapeutics as well as providing an understanding of innate immune signalling at the molecular level.

Due to the ability of A46 to inhibit all TLRs [46] a small library of peptide fragments derived from this protein sequence was tested for ability to inhibit TLR signalling [60]. One 11 aa peptide (KYSFKLILAEY) termed VIPER was reported to retain the inhibitory properties of full length A46 against TLR4 signalling [60]. A 9R homopolymer delivery sequence at the C

terminus provides delivery of the peptide into cells. Although A46 inhibits multiple TLRs by interacting with MyD88, TRIF, TRAM, and Mal, VIPER was shown to specifically inhibit only TLR4 and not IL-1 nor other TLRs. This suggests that A46 contains specific sites for interaction with each adaptor protein.

Lysakova-Devine et al. reported interaction of VIPER with Mal and TRAM using GST and His-tagged pull-down assays. However, more recently Oda et al. used SPR analysis, co-purification studies, and isothermal titration calorimetry to show that the affinity of VIPER for Mal may not be significant in vitro [57]. This may explain the previously reported lack of TLR2 signal inhibition by VIPER which also requires Mal for signal transduction [60].

As mentioned previously, A46 engages with adaptor TIR domains through its Bcl-2-fold. A model based on the A52 structure predicted the VIPER sequence to be on the surface of A46 [60]. This model situates the leucine critical to VIPER functionality on an electropositive surface portion of A46 which facilitates interaction with the predicted electronegative TIR domains of Mal and TRAM thought to interact with TLR4. However, the precise structure of these complexes remains to be defined.

Although the data from Oda et al. indicates that VIPER has low affinity for Mal, TLR4 signalling is still significantly reduced in the presence of the peptide [60]. There may be multiple factors contributing to the difficulty of identifying the mechanisms of inhibition. Mal functions in TLR2 signalling yet VIPER has been previously reported to cause no inhibition of this pathway. Mal is thought to bind to TLR4 and TLR2 via two different sites [2]. Discussed earlier, the Mal AB loop is suggested to mediate interaction with the TLR4

TIR domain BB loop [17]. In contrast, the Mal DD loop is likely to be more important for interaction with the TLR2 TIR domain [61, 62].

VIPER represents the first example of a short virally derived peptide inhibitor of a specific TLR signalling pathway. Not only does this offer insight into mechanisms of TLR signalling but may also provide therapeutic benefit since VIPER inhibits TLR4 signalling at much lower concentrations and with a lower molecular weight than comparable BB loop peptides [29, 30, 63]. TLR4 has roles in a number of conditions including sepsis [64], acute pancreatitis [65, 66], acute liver failure [67, 68], ischemia/reperfusion injury [69-71], rheumatoid arthritis [72], etc. Previously, control of autoimmune responses or sepsis focused on inhibition of proinflammatory cytokines such as TNF-α to prevent TLR4-mediated inflammation. Targeting TLR4 directly may be more efficient and reduce the offshoot effects of pervasive immune suppression.

1.12 Nuclear magnetic resonance spectroscopy

Nuclear magnetic resonance spectroscopy (NMR), is a technique that exploits the magnetic properties of certain atomic nuclei. When placed in a magnetic field, NMR active nuclei (such as 1H or 15N) absorb electromagnetic radiation at frequencies specific to the isotope of interest. A spinning charge of a proton generates a magnetic field that results in a magnetic moment proportional to the spin. In the presence of an external magnetic field, two spin states exist where one aligns with the magnetic field and the other opposes it. Irradiation of the sample with energy equal to the spin state separation of a set of nuclei will allow a transition of the lower energy state to a higher energy state.

The strength of the magnetic field determines the resonant frequency, energy of the absorption, and the intensity of the signal. For example, protons have a Larmor frequency of 21 MHz in a magnetic field of 0.5 Tesla. The sample is excited with a radio frequency pulse, to produce afree induction decay (FID) which is recorded for analysis. A Fourier transform is performed on the weak FID signal to extract the frequency-domain spectrum from the raw time-domain FID. The signal-to-noise ratio can be improved with repeated spectra acquisitions. However, for large peptides or proteins this can be time consuming.

Different resonant signals are observed for each spin system because of variations in the electromagnetic environments of the proton. Electron density around a nucleus shields it from the external magnetic field. The chemical shift is the resonant frequency of a nucleus relative to a standard.

For peptide structure investigations two-dimensional NMR methods are generally used, such as correlation spectroscopy (COSY) and total coherence transfer spectroscopy (TOCSY) to detect through-bond nuclear couplings. Nuclear Overhauser effect spectroscopy (NOESY) is used to detect couplings between nuclei that are close to each other in space.

1.13 Final summary

I have described the advances in the characterisation of TLR4 and its adaptor proteins. The current knowledge of structural interactions involved with TLR4 signalling complexes still has questions that remain unanswered. The timing and sequence of events for adaptor binding has been discussed and several models report a consensus on the endosomal evolvement of TRAM. The TRAM and Mal binding sites have not been fully identified. The mechanisms of A46 TLR inhibition with particular interest to A46 derived peptide VIPER have been

considered. Although capable of significantly reducing LPS mediated TLR4 signalling, VIPER not been previously reported to affect the response of activated TLR2. Several factors may contribute to this finding, including a lower affinity for Mal than TRAM, structural changes of the TLR4 TIR domain, adaptor proteins, and possibly to the viral peptide itself after binding, and the differing adaptor surface regions required for signalling by TLR2 and TLR4. Redundancy has also been shown for Mal which was previously considered critical for TLR2 signalling. VIPER offers greater therapeutic options than host derived BB loop peptides and it is possible to develop retro-inverso peptides to provide greater retention of bioactivity and stability than other drugs. The use of viral immune modulation can provide future insight into the complex systems involved in pathogen detection and inflammation.

The currently used bioactive form of VIPER (KYSFKLILAEYRRRRRRRRR) – consists of 11 amino acids that are derived from A46 and the 9 arginine residues act as a peptide transduction motif to allow VIPER to traverse the cell membrane. 9R-VIPER contains the transduction motif on its N terminus.The specific aims of this project are to;

Compare the ability of VIPER and 9R-VIPER to block TLR4 and TLR2 agonist responses in vitro.

Determine the longevity of TLR4 inhibition by VIPER and VIPER-derived peptides in vitro.

Compare wild type and peptides with muted residues predicted to be required for protein binding.

Determine the NMR structure of 9R-VIPER.

This information will be used to select optimal peptides for further in vivo efficacy studies. The NMR structure of these peptides will be applied in moving to design peptidomimetics

based on VIPER. Overall the project will contribute to the development of a novel virally-derived TLR4 inhibitor which may ultimately have use in TLR4-dependent human disease.

2.1 Materials

2.1.1 Cell culture

Murine wild-type immortalised bone marrow-derived macrophages (wt iBMDMs) were taken from liquid nitrogen stores and continually passaged until project completion. Human peripheral blood mononuclear cells (PBMCs) were purified from the buffy coats of heparinised whole blood preparation available for research use from the St. Jame's Hospital Blood Bank (Dublin, Ire).

2.1.2 Antibodies

Goat anti-mouse TNFα, biotinylated goat anti-mouse TNFα, recombinant mouse TNFα, mouse anti-human TNFα, biotinylated goat anti-human TNFα, recombinant human TNFα, mouse anti-human CXCL10/IP-10, biotinylated goat anti-human CXCL10/IP-10, and recombinant human CXCL10/IP-10 were all purchased from R&D Systems (MN, USA). Rabbit IgG anti-mouse interferon beta protein A (Milipore, CA, USA), polyclonal goat anti-mouse interferon beta (Milipore, CA, USA), recombinant mouse interferon beta (biolegend, SD, CA, USA).

2.1.3 Receptor agonists

Ultrapure LPS from gram-negative bacteria (*Escherichia coli)* (> 99% pure in respect to DNA, proteins and TLR2 agonist contents) was purchased from Alexis Biochemicals (Nottingham, UK). Malp-2 and Pam3Csk4 were purchased from Invivogen (San Diego, CA, USA).

Most of the remaining standard laboratory chemicals were purchased from Sigma-Aldrich (Dublin, Ire).

2.2 Methods

2.2.1 Cell culture

Wt iBMDM were grown in Dulbecco's Modified Eagle's Medium (DMEM) supplemented with 10% (v/v) hear inactivated foetal bovine serum (FBS), 2mM L-glutamine and 100µg/ml gentamicin (further referred to as complete medium). Human PBMC were cultured after purification in RPMI medium broth supplemented with with 10% (v/v) FBS and 10 mg/ml ciprofloxacin. Cells were kept in a 37^{o} C incubator with a humidified atmosphere of 5% CO_2. Wt iBMDM were subcultured once confluencies of 60-80% were achieved (2-3 days). Adherent wt iBMDM were scraped from flask surfaces after washing with complete medium. Re-seeding was performed with warmed medium. Cell counting was performed using a haemocytometer under a light microscope before seeding into appropriate experimental vessels at the desired concentrations.

Buffy coats were collected from heparinised blood. From this human PBMCs were isolated by density centrifugation using Lymphoprep. Heparinised blood was diluted (2:1) with sterile 1x Phosphate-buffered Saline (PBS) (137 mM NaCl, 2.7 mM KCl, 10mM Na2HPO4, 2mM NaH2PO4). 45ml was transferred into 50ml a Falcon tube and centrifuged at 4000rpm for 20 min. The layer of white blood cells formed at the interface between red blood cells and serum was carefully transferred onto a new 50ml Falcon tube containing 15ml Lymphoprep. The total volume was brought to 50ml with sterile 1x PBS if required. Citrifugation was applied at 1200rpm for 20 min. The top layer was carefully removed and PBMCs were

collected from the subsequent layer taking care to avoid the remaining layer of Lymphopred/red blood cells. Isolated PBMCs were washed 3-4 times in sterile 1x PBS, counted and seeded at a density of $1x10^6$ cells/ml in complete RPMI in appropriate experiment vessels.

2.2.2 Peptide synthesis and reconstitution

Peptides were ordered to specification from GenScript Corporation (Centennial Ave, Piscataway, NJ, USA) with a reported purity of > 95% as determined by HPLC and MS. FlexPeptide™ technology was used for peptide synthesis and delivered as a lyophilised powder. The peptide powder was reconstituted in molecular biology grade water from Sigma-Aldrich. 10mM working dilutions were prepared and stored at -20^o C. Working stocks were prepared from this at concentrations of 100µM, 500 µM, and 2mM. A 2 µl treatment to 200 µl cell culture wells provided total concentrations of 1, 5 and 20 µM respectively.

Table 2.1 Peptide Sequences

VIPER	KYSFKLILAEY
9R-VIPER	9R-KYSFKLILAEY
9R-VIPER L6A	9R-KYSFKAILAEY
9R-VIPER L6AE10A	9R-KYSFKAILAAY
CP7	RNTISGNIYSA-9R

2.2.3 Enzyme-Linked ImmunoSorbent Assay (ELISA)

Cytokine responses to cell culture treatments were dertermined by performing Enzyme-Linked ImmunoSorbent Assays (ELISA). MaxiSorp® flat-bottom 96 well plates were coated with 50 µl/well capture antibody which had been diluted to the required concentration in

sterile 1x PBS and stored overnight at 4^{o} C. Plates were then washed 3 times in 0.5% (v/v) PBS-Tween 20 and excess dried by blotting on clean dry paper. Plates were then blocked for 1 hour with reagent diluent (0.05% FCS- 1x PBS for mTNFα, hTNFα, and hIP-10, or 0.05% FBS- 1x PBS for mIFNβ). Plates were washed as before. Samples were added to wells and diluted if necessary in reagent diluent at a total volume of 50 µl/well. Standards were prepared to concentrations of 2000 pg/ml and plated at the same time as samples. Samples and standards were stored a minimum of 2 hrs at 37^{o} C or at maximum overnight at 4^{o} C. Plates were washed as before. Detection antibody was added at the required concentration in reagent diluent and incubated at a minimum of 2 hrs at 37^{o} C or at maximum overnight at 4^{o} C. Plates were washed as before. After washing 50 µl/well of horseradish peroxidase (HRP), diluted as per manufacturer's instructions in reagent diluent, was added and incubated at room temperature away from direct light for 20 min. After the final wash, 50 µl/well of substrate reagent mixture (1:1) was added and incubated 10-20 min. 50 µl/well of stop solution (1M H_2SO_4) was used to stop the reaction and colour development was read on a Multiscan Accent spectrometer (BioSciences, Ire) at $\lambda = 450$ nm.

Table 2.2 ELISA capture and detection antibody dilution factor

Antibody	Capture	Detection	Sample Dilution
mTNFα	1 : 125	1 : 180	25
mIFNβ	1 : 1000	1 : 2000	1
hTNFα	1 : 180	1 : 180	9
hIP-10	1 : 180	1 : 180	1

2.2.4 MTT assay

MTT (3-[4, 5-*dimethyl*-2-thiazolyl] -2, 5-diphenyl -2H- tetrazolium bromide) assay was used to determine the viability of cells after appropriate experiments. MTT (Sigma-Aldrich) was reconstituted in PBS to a concentration of 1 mg/ml. After supernatant had been fully removed from 96 well culture plates cells were washed once using 200 µl / well 1x PBS. PBS was discarded by inverting plate and blotting on clean paper. 200 µl /well of 1mg/ml MTT solution was added directly to cells which were then incubated for 2 hrs at 37^{o} C. After 2 hrs, the MTT solution was pipetted off and the remaining crystals were dissolved with 200 µl / well of DMSO solution by incubating 20 min at 37^{o} C. Plates were read on a spectrometer at $\lambda = 595$ nm.

2.2.5 Statistical analysis

Statistical analysis were carried out using unpaired Student's t-test. The data are expressed as mean ± SD of triplicate samples and representative of three independent experiments unless otherwise stated. Graphs and analysis of cell culture assay were carried out using Graphpad Prism.

2.3 NMR analysis

NMR data for chemical shift assignments were collected using 600 and 800 MHz specetromoeters and pH 4.5. A 2mM concentration of 9R-VIPER was analysed in a volume of 300 ml H_20 with 10% D_20. 9R-VIPER L6E10A was analysed at a concentration of 5mM in a volume of 150 ml H20 with 10% D_20.

2.3.1 NMR Experiments

HN-HSQC 60ms, HC-HSQC 60ms, TOCSY 60 ms, NOESY 60ms, COSY 60ms, NOESY 150 ms. Other data was collected but not used for sequence assignment.

2.3.2 Pulse sequence details for MNR data acquisition

TOCSY 60 ms

Homonuclear Hartman-Hahn transfer using MLEV17 sequence for mixing, using two power levels for excitation and spinlock,phase sensitive, water suppression using watergate W5 pulse sequence with gradients using double echo [73, 74].

NOESY 60ms

2D homonuclear correlation via dipolar coupling (dipolar coupling may be due to noe or chemical exchange), phase sensitive water suppression using watergate W5 pulse sequence with gradientsusing double echo allowing for presaturation during relaxation delay in cases of radiation damping [74].

HN-HSQC

2D H-1/X correlation via double inept transfer using sensitivity improvement of phase sensitive Echo/Antiecho-TPPI gradient selection. Decoupling during acquisition accounted for by using trim pulses in inept transfer using f3 – channel with gradients in back-inept [75-77].

The mutant peptide9R-VIPER L6AE10A was also investigated using TOCSY as described previously with a mixing time of 150 ms.

2.3.3. NMR peak assignment

Assignment panel reference table was used to compared identified chemical shifts at pH: 4.5, Temp, 298 K [78]. Atom types included in NOESY, TOCSY, HC-HSQC, and HN-HSQC

were HN, HA, HB1, HB2, CA, CB, C, and N. Assignments were carried out using TOPSPIN (Bruker) and NMRViewJ (OneMoon Scientific) software.

3. Results

3.1.1 9R-VIPER has greater inhibitory properties than VIPER for LPS driven TNFα in both wt iBMDM and human PBMC

The peptide VIPER, derived from the VACV protein A46, has been previously shown to block TLR4-dependent gene induction. To test if the inhibitory properties of VIPER were dependent on the position of the 9R delivery sequence, VIPER and CP7 were synthesised with a C-terminus 9R delivery sequence and compared to 9R-VIPER which contained an N-terminus delivery sequence. Peptides were tested at a range of concentrations in both murine wt iBMDM and human PBMC. Cells were seeded (PBMC at $1x10^6$ cell/ml and BMDM at $5x10^5$ cell/ml) 24hrs before treatment. Peptides were added at concentrations of 1, 5 and 20 μM at a volume of 2 μl 1 hour before stimulation with 100 ng/ml LPS. Unstimulated wells were treated with identical peptide concentrations to monitor for peptide-dependent toxicity or any non-specific affects due to the modified peptide sequences. Experiments were performed with harvesting at both 3 and 24 hrs after LPS stimulation.

Figure 3.1.1 A, shows that in wt iBMDM 9R-VIPER is more effectively inhibits LPS induced TNFα production at a 5 μM concentration. Similar results are shown after 24hrs (Figure 3.1.1 B) where concentrations of both 5 and 20 μM 9R-VIPER have greater inhibitory properties than VIPER. Figure 3.1.2 shows the affect on cell viability determined by MTT. Some toxicity is indicated when a 20 μM is used in iBMDM with a 50% reduction in viability.

In human PBMCs 9R-VIPER was more effective than VIPER at a concentration of 20 μM. Figure 3.1.4 B indicates that unlike wt iBMDM, little variance is seen in human PBMC cell viability under any of the conditions tested. In PBMCs 20 μM 9R-VIPER is more effective than the same concentration of VIPER (FIGURE 3.1.3 A). 20 μM is the optimum

concentration for signal inhibition in PBMC whereas 5 μM is sufficient in wt iBMDM (Figure 3.1.1 B). To investigate further, multiple human samples were tested different concentrations. Six separate donors were treated with 20 μM VIPER and 9R-VIPER At this concentration 9R-VIPER was more effective at blocking LPS driven TNFα than VIPER (Figure 3.1.4). 5 μM was also tested (see Figure 3.1.6 A) although this concentration did not yield as precise inhibition between donors as did the higher dose.

3.1.2 9R-VIPER has greater inhibitory properties than VIPER for LPS driven IFNβ in wt iBMDM

Experiments were performed identically as those reported in figure 3.1.1 B. The induction of IFNβ was inhibited almost completely at the optimum 9R-VIPER concentration of 5 μM (Figure 3.1.5 A). Although not as effective as 9R-VIPER, VIPER with the C-terminus delivery sequence produced a > 6 fold reduction in LPS driven IFNβ.

3.1.3 9R-VIPER and VIPER inhibit for LPS driven IP-10 equally well in PBMC

To investigate the ability of VIPER and 9R-VIPER to inhibit IFN inducible genes in humans, multiple donors were used for testing with both 5 and 20 μM peptide concentrations. As in Figure 3.1.1 B, 100 ng/ml LPS was used to drive TLR4-dependent IP-10. The optimum concentration of peptide in PBMC, 20 μM (as reported in Figure 3.1.3 A), was shown to cause complete inhibition of IP-10 production using both VIPER and 9R-VIPER (Figure 3.1.5 B). 5 μM of both VIPER and 9R-VIPER was also effective in preventing expression of IP-10. This is in contrast Figure 3.1.3 A where 5 μM is not as effective as a 20 μM concentration of either peptide in PBMC inhibition of LPS driven TNFα.

3.2.1 VIPER and 9R-VIPER reduce TLR2-driven TNFα in wt iBMDM and PBMC

VIPER and the N-terminus polyarginine peptide, 9R-VIPER, were used to investigate the production of TLR2 driven TNFα. WT iBMDM were seeded at at $5x10^5$ cell/ml 24hrs before treatment with peptides of concentrations of 1, 5 and 20 μM delivered at a volume of 2 μl. 1 hour after peptide treatment cultures were stimulated with 20 nM of the TLR2/6 agonist Malp-2. Supernatants were harvested after 24 hrs. A dramatic difference was seen in the inhibitory capability of 9R-VIPER compared to VIPER at a 1 μM concentration (Figure 3.2.1 A). VIPER had little affect on Malp-2 driven TNFα at 1 μM, whereas 9R-VIPER treatment showed a 9-fold reduction in cytokine response. At 5 and 20 μM both VIPER and 9R-VIPER performed similarly with approximately 18-fold reduction in TNFα secretion. Malp-2 was selected for use at a concentration of 20 nM after performing a dose response in iBMDM (Figure 3.2.4). This was thought to provide stimulation to a level approaching that of LPS induced TNFα without causing oversaturation. Difficulties arose in replicating this finding consistently. Although it is out of the scope of this investigation, it may be interesting to determine the inhibitory properties of 9R-VIPER during TLR2 dose dependent stimulation. It is possible that stimulation with Malp-2 and the TLR2/1 agonist Pam3Csk4 at concentrations of 1, 5 and 20 nM may reveal differences in adaptor protein involvements during high and low dose exposure.

To investigate TLR2 driven TNFα inhibition in human PBMC cells were seeded at $1x10^6$ cell/ml and treated identically to the iBMDM already mentioned. Figure 3.2.1 B shows that with 6 individual donors, both peptides reduced TNFα production in a repeatable manner with 9R-VIPER showing slightly better inhibition.

3.2.2 9R-VIPER has greater inhibitory properties than VIPER for Malp-2 driven IFNβ in both wt iBMDM and human PBMC

The TLR2 – IFNβ signalling pathway was introduced in section 1.7. Many of the details surrounding this pathway remain to be elucidated. Here, I investigated both the induction of TLR2-dependent IFNβ and subsequently, its inhibition by VIPER and 9R-VIPER. As mentioned previously, agonist concentration is a concern for this process. 20 nM Malp-2 was used here, although a lower dose of 2-10 nM may give more precise results if revisited in the future. TLR2-driven IFNβ was investigated in an identical manner to TLR2-driven TNFα in wt iBMDM. At its lowest dose (1 μM) 9R-VIPER was shown to be as effective as the high dose VIPER (20 μM) at reducing Malp-2 driven IFNβ (Figure 3.2.2 A). The finding of Malp-2 driven INFβ inhibition by VIPER correlates with recent work by Stack et al. (data unpublished), although here 9R-VIPER was found to be more effective than VIPER at each concentration tested.

9R-VIPER's capability against TLR2-driven IP-10 was tested in human PBMC with 4 individual donors under the same conditions although cells were seeded at $1x10^6$ cell/ml. 20 nM Malp-2 caused poor induction of IP-10 relative to unstimulated controls (Figure 3.2.2 B). However, in donors treated with 20 μM peptide, both VIPER and 9R-VIPER retained IP-10 production at basal levels, with 9R-VIPER showing greater inhibitory capacity overall. Figure 3.2.3 shows inhibition by both 5 μM VIPER and 9R-VIPER relative to controls, although fewer donors have been reported at this treatment concentration. Overall, both induction of TLR2 stimulated IFNβ was achieved and subsequently shown to be inhibited by 9R-VIPER more potently than VIPER.

3.3 9R-VIPER peptide residues required for effective TLR4 signal inhibition in wt iBMDM and human PBMC

Previous studies have identified residues which may be required for efficient adaptor protein binding. Choe et al. recently reported A46 surface residues of the VIPER peptide which, when mutated reduce the activity of A46. Due to the success of 9R-VIPER in all previous sections, this peptide form was chosen for studies of residue essentiality to biological activity. Leucine 6 and Glutamic acid 10 of the VIPER sequence are believed to be required for interaction with adaptor protein surfaces. Mutant peptides were synthesised by replacing these amino acid residues with alanine residues by GenScript (NJ, USA). Mutants of 9R-VIPER E10A and 9R-VIPER L6AE10A were produced, while great difficulty was encountered in producing the second, single residue mutant 9R-VIPER L6A. Therefore studies were conducted using the single mutant E10A and double mutant L6AE10A.

Wt iBMDM cells were seeded at $1x10^5$ cell/ml 24hrs before treatment. Peptides were added at concentrations of 1, 5 and 20 μM at a volume of 2 μl 1 hour before stimulation with 100 ng/ml LPS. Supernatants were harvested after 24hrs.

In wt iBMDM, 9R-VIPER, as reported in earlier sections (Figure 3.1.1 B), caused significant reduction in LPS-driven TNFα at concentrations of 5 and 20 μM peptide. Almost identical responses were shown by the E10A mutant indicating no loss of function (Figure 3.3.1 A). In comparison the double mutant L6AE10A showed major loss of function at the 5 μM concentration with a 7-fold reduction of inhibitory capacity. At the higher concentration of 20 μM L6AE10A had less loss of function although still a1.5-fold difference to that of 9R-VIPER. As reported earlier (Figure 3.1.2), in iBMDM, 5 μM peptide treatment indicates the most accurate results repeatedly without concerns for cell viability.

To test this finding in human PBMC, cells were treated and stimulated in the same fashion as iBMDM (except seeded at 1x106 cell/ml) and supernatants harvested after 24hrs. Peptide was delivered at concentrations of 1, 5 and 20 μM at a volume of 2 μl without concern for cell viability as described earlier (Figure 3.1.3 B). In PBMC 20 μM is considered the ideal concentration of 9R-VIPER for TLR4-induced TNFα inhibition (Figure 3.1.3 A-B). At this concentration almost complete loss of function as found in the double mutant L6AE10A compared to no loss of function in the same concentration of single mutant E10A (Figure 3.3.1 B). Complete loss of function was shown for 5 μM concentration of the double mutant L6AE10A.

By conducting these experiments comparing 9R-VIPER and the mutant peptide, residues L6 and E10 are shown to play an import role in the interface of 9R-VIPER and its binding targets during TLR4-driven TNFα responses in iBMDM. However, the second single mutant (L6A) is needed to accurately confirm the requirement of both residues L6 and E10 in binding and inhibiting TLR4 adaptor proteins. Although, evidence from the structural changes in the double mutant L6AE10A compared to 9R-VIPER (described later) predicts that both residues are at least required for the necessary secondary structure confirmation to allow successful binding interactions with its adaptor protein targets Mal and TRAM.

3.4 Longevity of TLR4 inhibition by VIPER and 9R-VIPERin wt iBMDM and human PBMC

To compare the longevity of VIPER and 9R-VIPER activity in cell culture, wt iBMDM (seeded at $1x10^5$ cells/ml) were treated with 5 μM of peptide at intervals of 1, 12 and 24 hours prior to 100 ng/ml LPS stimulation. Supernatants were harvested 3 hours after LPS stimulation.

Figure 3.4.1 shows that treatment 24hrs prior to stimulation results in poor inhibition of LPS-driven TNFα in both VIPER and 9R-VIPER compared to untreated controls. VIPER retained little inhibitory activity when treatment was provided 12 hours prior to stimulation. At the same time point 9R-VIPER retained some of its inhibitory properties although this was only a 56% reduction in TNFα compared to CP7 and normalised against the unstimulated control. When treatment was provided at 1 hour prior to stimulation both VIPER and 9R-VIPER retained the inhibitory properties reflected in Figure 3.1.1 B with 9R-VIPER showing significantly greater inhibition than VIPER at a 5 μM concentration.

Figure 3.4.2 reports the activity of VIPER and 9R-VIPER when treatment was applied 1 hour prior to stimulation and harvested 3 and 24 hrs after stimulation. At both times points 9R-VIPER demonstrates significantly greater inhibition of LPS induced TNFα production than VIPER at a 5 μM concentration.

These results indicate that although 9R-VIPER demonstrates greater biological activity than VIPER towards inhibition of TLR4 mediated TNFα, the level of inhibition is reduced dramatically if the peptide is delivered several hours prior to stimulation. However, once stimulation occurs, activity of peptide present in the system retains cytokine expression at a consistently low level. Again, 9R-VIPER demonstrated significantly greater activity than VIPER after 3 and 24 hrs of stimulation when treatment was delivered1 hour prior.

3.5 NMR determination of peptide structure

3.5.1 9R-VIPER structure

Assignment of 9R-VIPER Nitrogen – proton interaction was based on HN-HSQC spectra. TOCSY, NOESY, HC-HSQC assignments allowed for the identification of a partial α-helix from the N-terminus of the VIPER sequence (after 9R) until residue 9, alanine. TOCSY spectrum yielded through bond correlations via spin-spin coupling which were combined with Nuclear overhauser effect (NOE) observations by NOESY. These methods allowed the identification of a β-sheet like tail occurring for residues 10-11.

Of particular note is the aromatic side chain of Tyrosine residue 11 which folds back along the outside of the helix and interacts with residues 4 and 6. The proton γ1 of the Tyrosine side chain cross peaks with amide proton of Phenylalanine 4. The proton γ of Luecine 6 is also seen to share interactions with Tyrosine 11 proton α.

The aliphatic Leucine 6 and the acidic Glutamic acid 10 are thought to be required for interaction with adaptor proteins Mal and TRAM. NOESY assignment indicates that these residue side chains are solvent exposed and available for binding in 9R-VIPER.

3.5.2 9R-VIPER mutant L6AE10A structure

Because of the success in showing loss of TLR4 signal inhibition when peptide residues were mutated, the mutant peptide 9R-VIPER L6AE10A was also analysed on an 800 MHz spectrometer. HN-HSQC was compared to that of 9R-VIPER. Initially the peaks seemed to overlap almost completely. TOCSY assignment was required to identify that HN-HSQC peaks were significantly shifted from those of 9R-VIPER for about 40% of residues, with apparent similarity in peak values due to overlap.

As expected, the residue substitutions of L6 and E10 to alanines made assignment of side chains easier because of reduced overlap (since alanine contains only a single methyl side chain). Surprisingly the 3D structure was more uniformly α-helical than that of 9R-VIPER. This difference was found to be due to the lack of glutamic acid 10 and leucine 6. Since the proton γ of luecine 6 is coupled to Tyrosine 11 proton α in 9R-VIPER this causes tension in the helix and also facilitates the hydophobicity of the aromatic side chains of both tyrosines at terminal ends of the sequence as well as the central phenylalanine. This activity is not present in the mutant peptide.

It is possible that the overall reduction in NOE occurring by though-space bonding between long amino side chains causes a more relaxed state with the overall structure dependent on spin coupling and interactions between shorter substituents.

These findings would indicated that 9R-VIPER retains an α-helical structure from the polyarginine N-terminus until a β-sheet like confirmation is taken by the three C- terminal residues, alanine, glutamic acid, and tyrosine. The long side chains of leusine and tyrosine cause the structure to bend and therefore expose the side groups of residues L6 and E10, which are shown to be in a proximity of at least 5Å with their proton δ.
When compared with the confirmation of VIPER in the A46 protein inferred by Kim et al. [79] the most significant difference is the change in the C-terminal confirmation and the orientation of tyrosine 11 (Kim et al tyrosine is shown as wireframe in Figure 3.5.1).

Figure 3.5.1 Is a cartoon representation of the 9R-VIPER 3D structure based on NRM data which was compiled in an assignment table and reference against expected chemical under the same circumstances as experimentation [78].

Figures

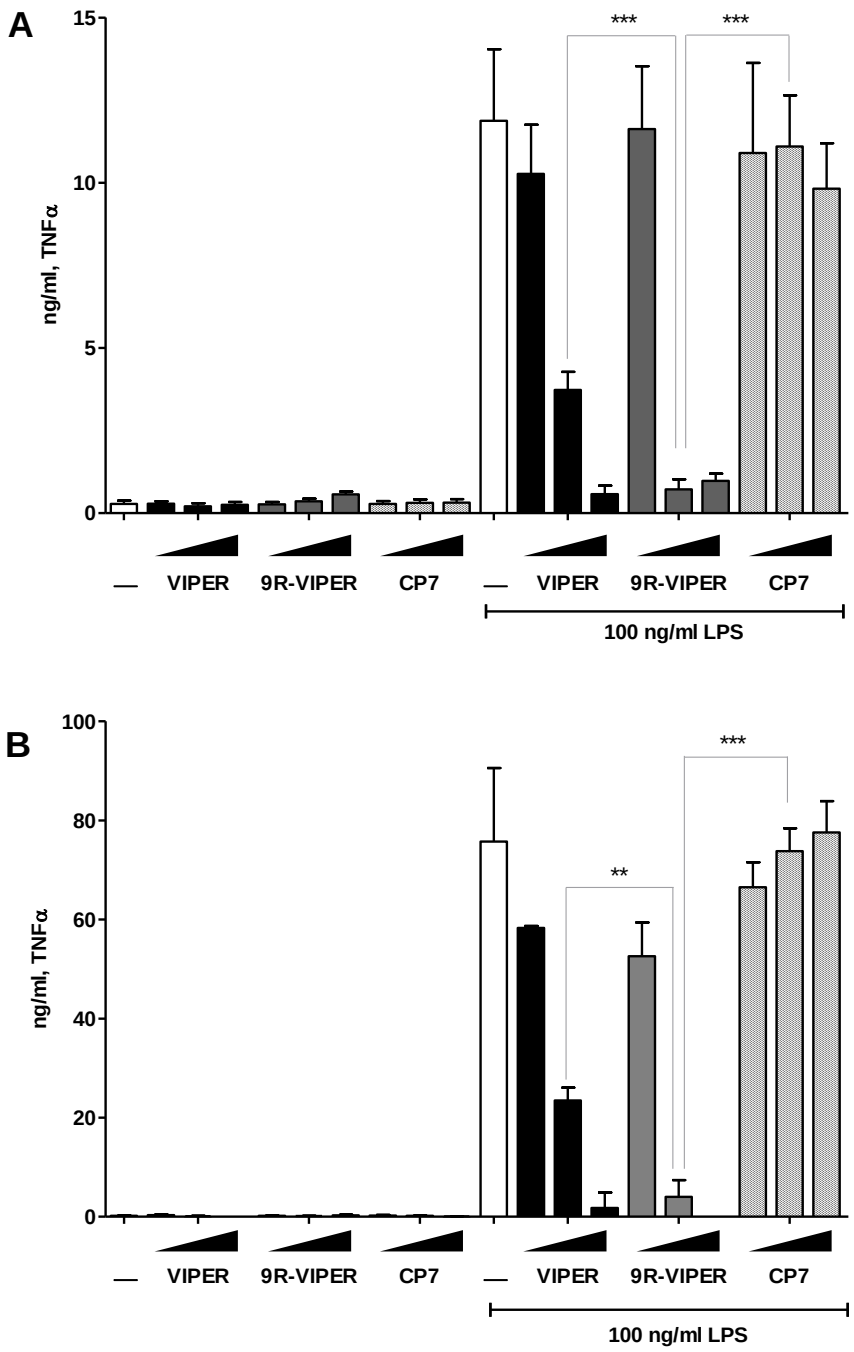

3.1.1 Inhibitory properties of 9R-VIPER and VIPER for LPS driven TNFα in wt iBMDM. Cells were trated with peptides VIPER, 9R-VIPER and CP7 at concentrations of 1, 5 and 20 μM 1 hour before stimulation with 100 ng/ml LPS. Supernatants were harvested after (**A**) 3 and (**B**) 24 hours and assayed for TNFα by ELISA.

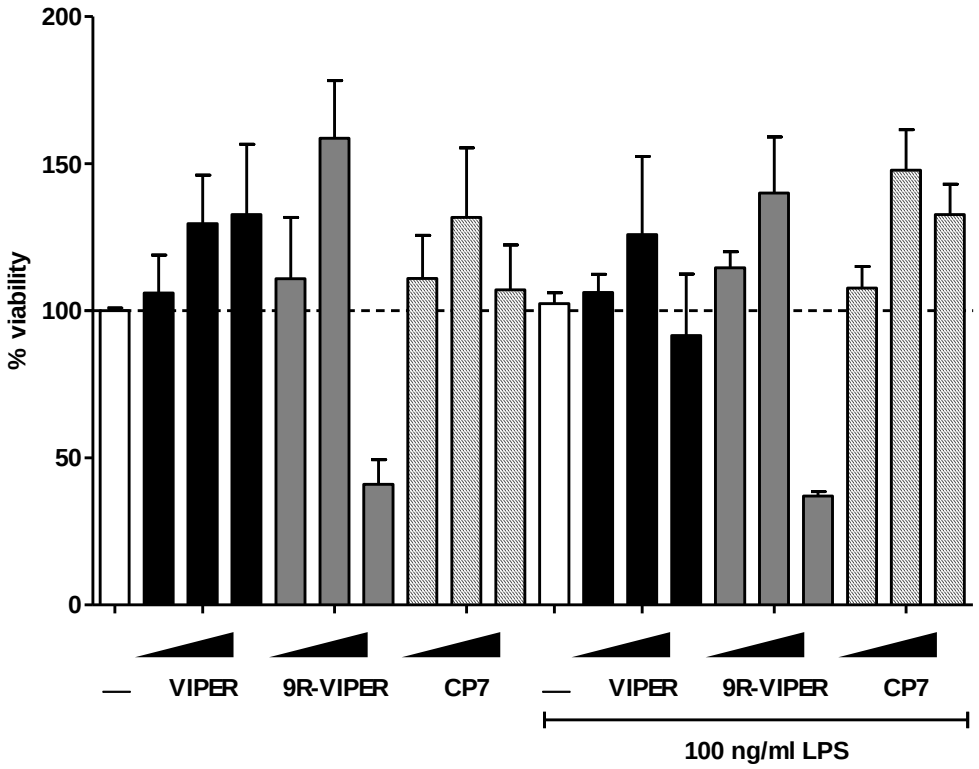

3.1.2 Affect on cell viability determined by MTT. After supernatant collection, cells from 3.1.1 were assayed for cell viability by treated with 1 mg/ml MTT for 20 min at 37^{o} C. Crystals were dissolved using DMSO and analysed at $\lambda = 595$ by spectroscopy.

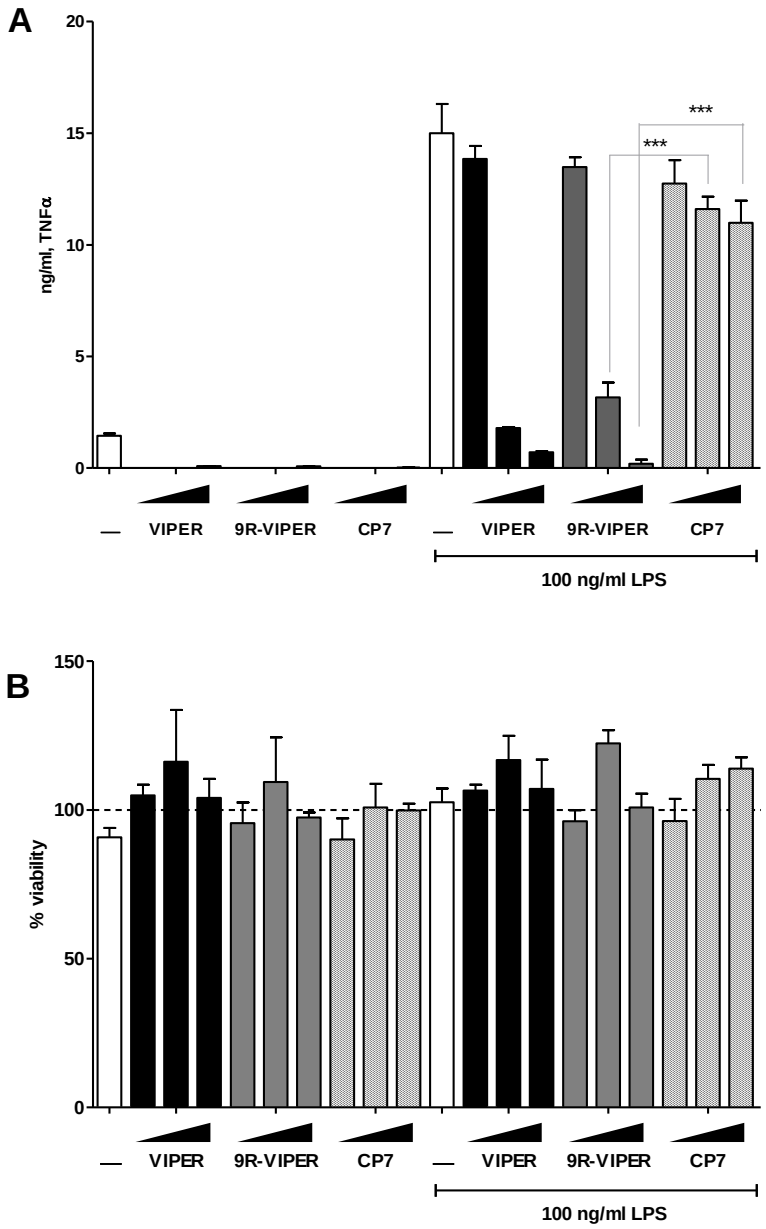

3.1.3 Inhibitory properties of 9R-VIPER and VIPER for LPS driven TNFα in human PBMC. A. Cells were trated with peptides VIPER, 9R-VIPER and CP7 at concentrations of 1, 5 and 20 μM 1 hour before stimulation with 100 ng/ml LPS. Supernatants were harvested after 24 hours and assayed for TNFα by ELISA. **B.** Affect on cell viability determined by MTT.

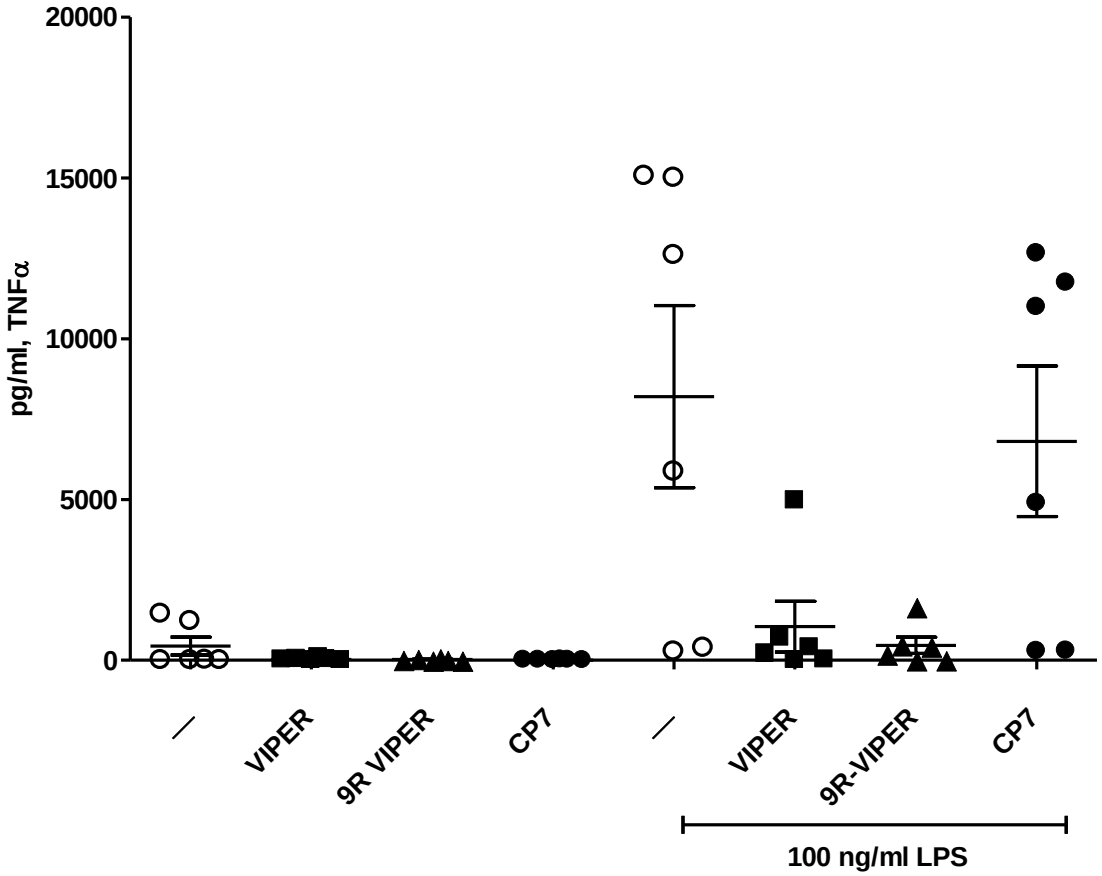

3.1.4 Inhibitory properties of 20uM 9R-VIPER and VIPER for LPS driven TNFα in human PBMC. Six separate donors were treated with 20 μM VIPER, 9R-VIPER and CP7 1 hour before stimulation with 100 ng/ml LPS. Supernatants were harvested after 24 hours and assayed for TNFα by ELISA.

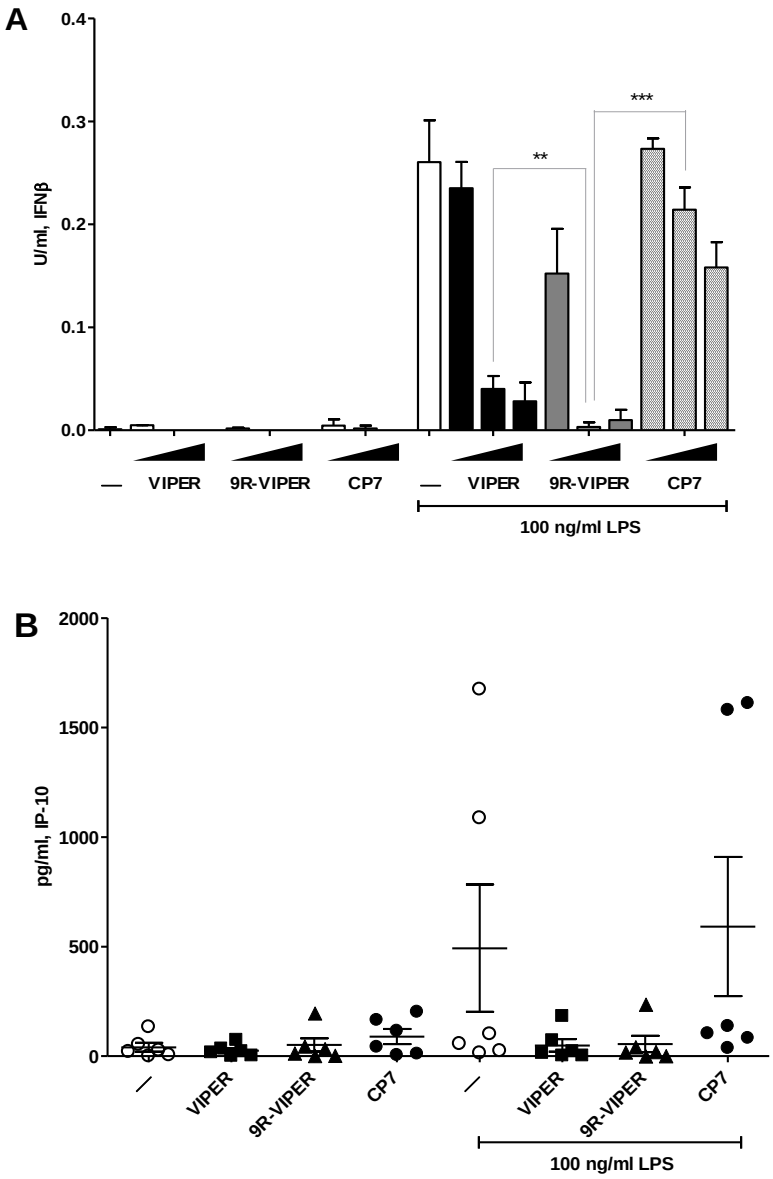

3.1.5 Inhibitory properties of 9R-VIPER and VIPER for LPS driven IFNβ in wt iBMDM and LPS driven IP-10 in PBMC. A. Wt iBMDM were trated with peptides VIPER, 9R-VIPER and CP7 at concentrations of 1, 5 and 20 μM 1 hour before stimulation with 100 ng/ml LPS. Supernatants were harvested after 24 hours and assayed for IFNβ by ELISA. **B.** Six separate donors were treated with 20 μM VIPER, 9R-VIPER and CP7 1 hour before stimulation with 100 ng/ml LPS. Supernatants were harvested after 24 hours and assayed for IP-10 by ELISA.

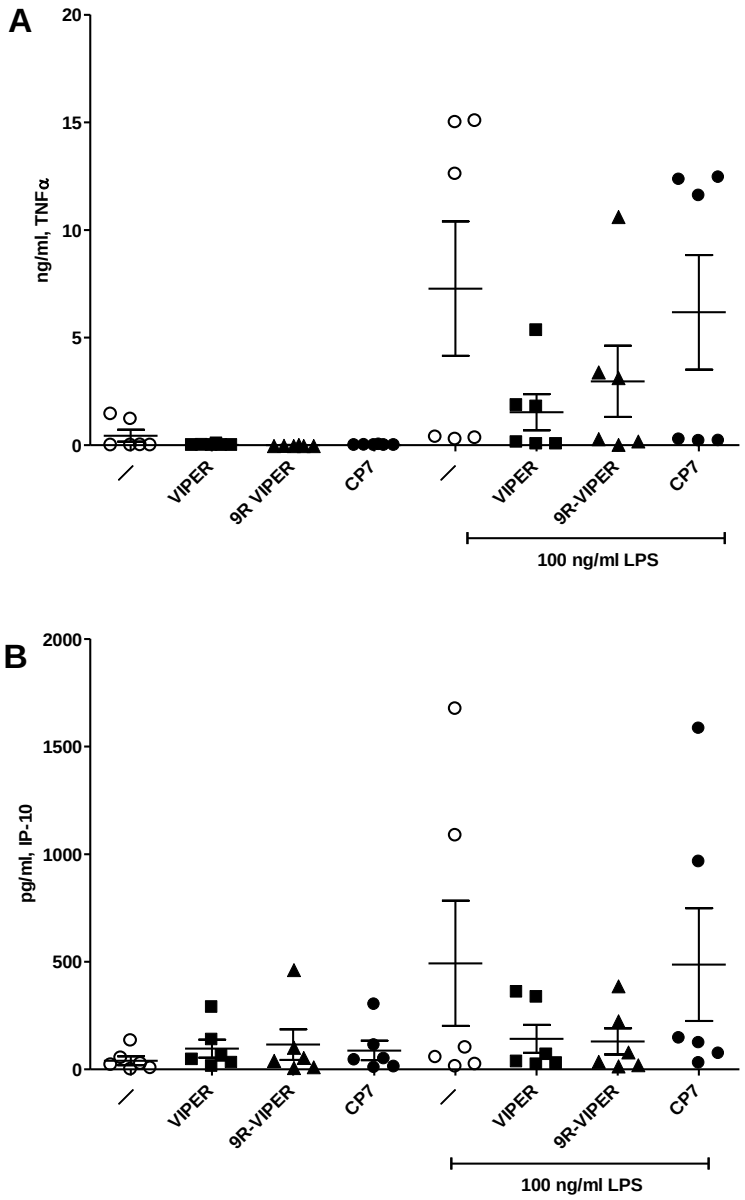

3.1.6 Inhibitory properties of 5 μM 9R-VIPER and VIPER in human PBMC. A. Six separate donors were treated with 5 μM VIPER, 9R-VIPER and CP7 1 hour before stimulation with 100 ng/ml LPS. Supernatants were harvested after 24 hours and assayed for TNFα by ELISA. **B**. Six separate donors were treated with 5 μM VIPER, 9R-VIPER and CP7 1 hour before stimulation with 100 ng/ml LPS. Supernatants were harvested after 24 hours and assayed for IP-10 by ELISA.

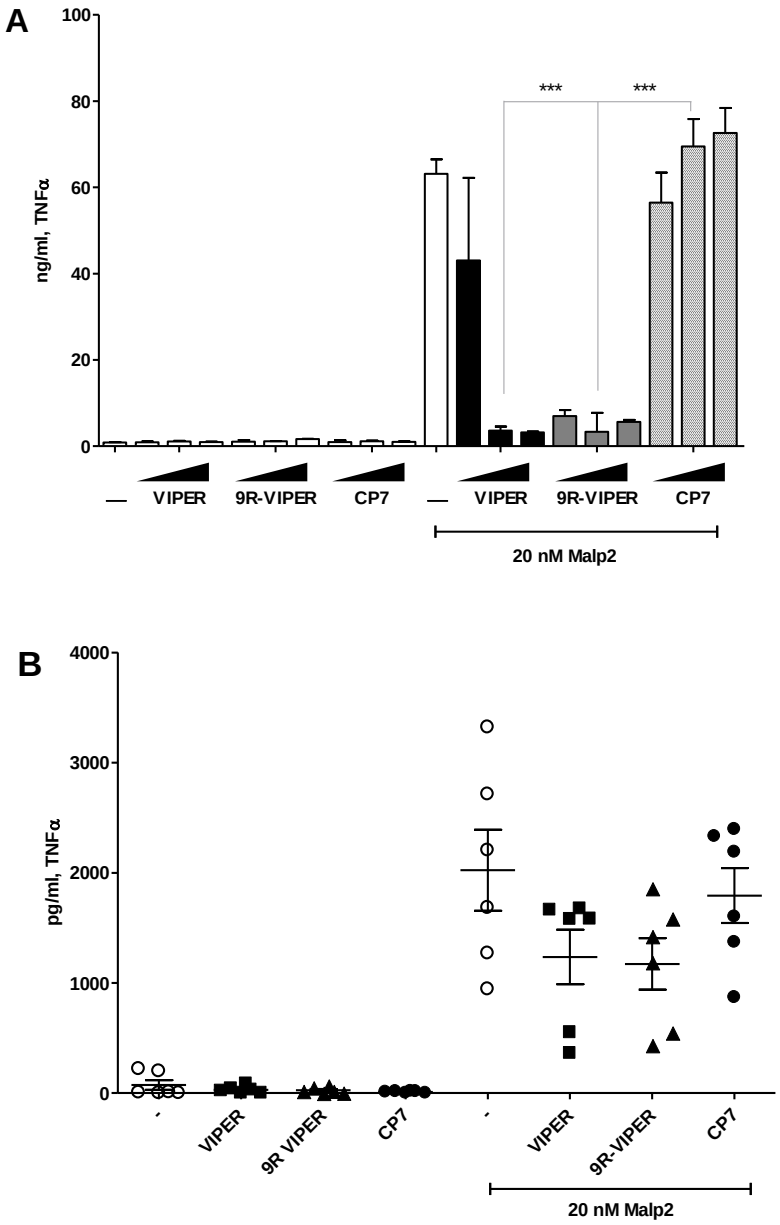

3.2.1 Inhibitory properties of 9R-VIPER and VIPER for Malp-2 driven TNFα in wt iBMDM and human PBMC. A. Wt iBMDM were trated with peptides VIPER, 9R-VIPER and CP7 at concentrations of 1, 5 and 20 μM 1 hour before stimulation with 20 nM Malp-2 (TLR2 agonist). Supernatants were harvested after 24 hours and assayed for TNFα by ELISA. **B.** Six separate donors were treated with 20 μM VIPER, 9R-VIPER and CP7 1 hour before stimulation with 20 nM Malp-2. Supernatants were harvested after 24 hours and assayed for TNFα by ELISA.

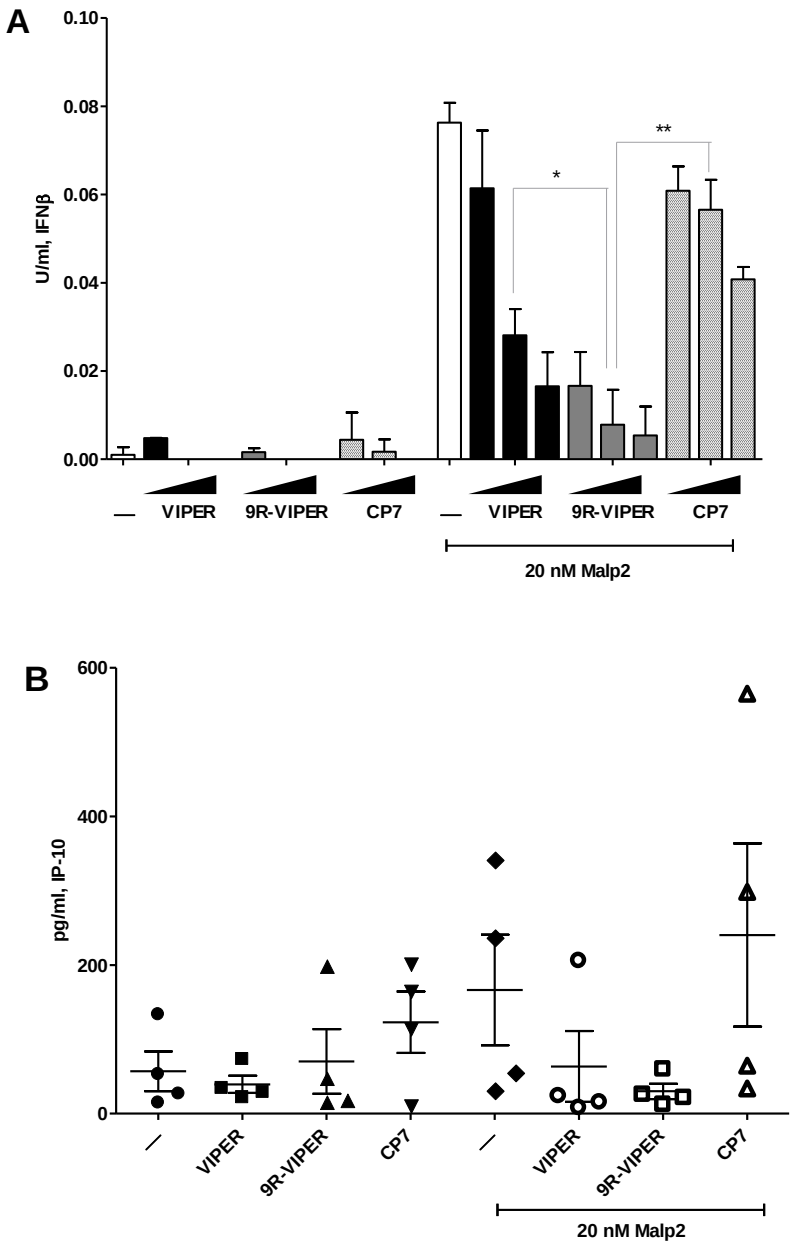

3.2.2 Inhibitory properties of 9R-VIPER and VIPER for Malp-2 driven IFNβ in wt iBMDM and Malp-2 driven IP-10 in PBMC. A. Wt iBMDM were trated with peptides VIPER, 9R-VIPER and CP7 at concentrations of 1, 5 and 20 μM 1 hour before stimulation with 20 nM Malp-2. Supernatants were harvested after 24 hours and assayed for IFNβ by ELISA. **B.** Four separate donors were treated with 20 μM VIPER, 9R-VIPER and CP7 1 hour before stimulation with 20 nM Malp-2. Supernatants were harvested after 24 hours and assayed for IP-10 by ELISA.

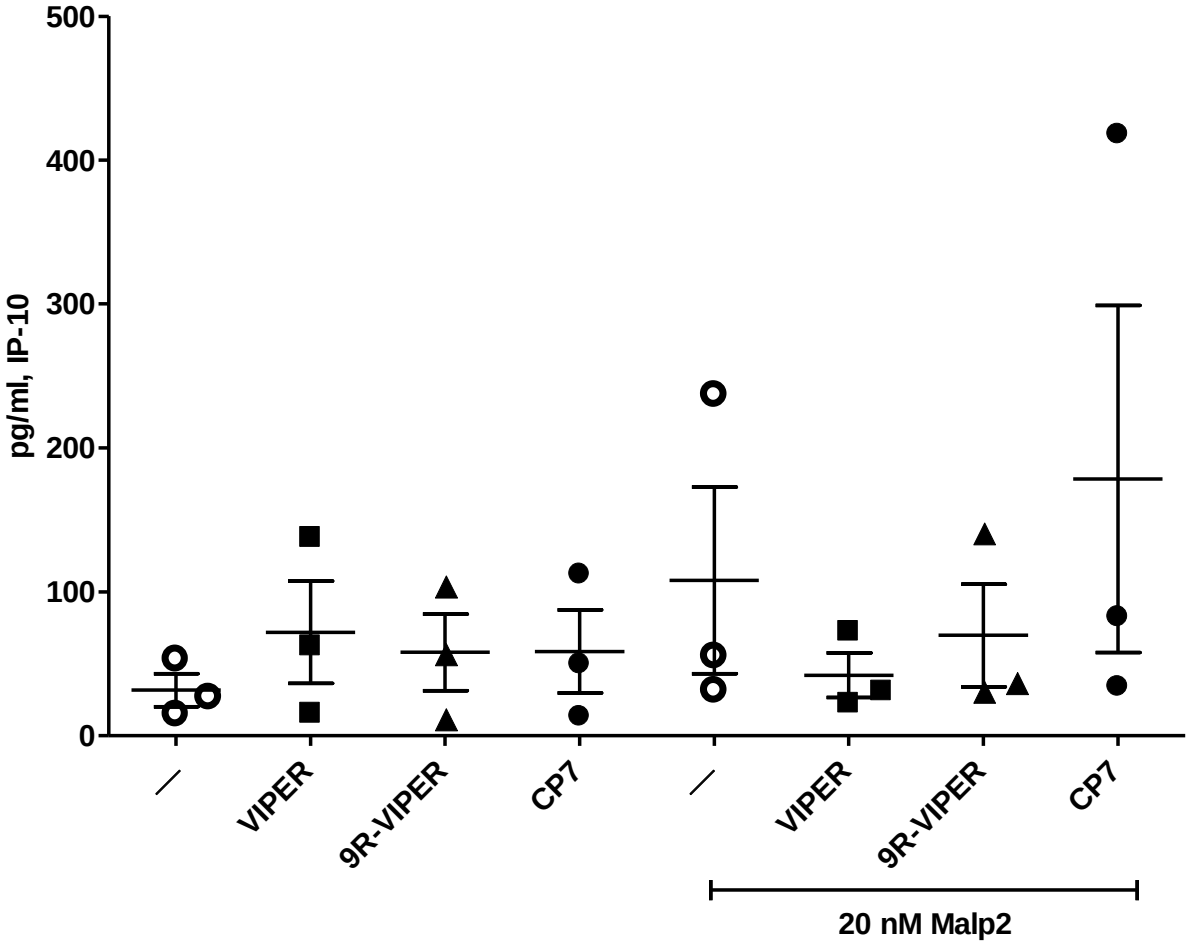

3.2.3 Inhibitory properties of 5 µM 9R-VIPER and VIPER for Malp-2 driven Malp-2 driven IP-10 in PBMC. **B**. Three separate donors were treated with 20 µM VIPER, 9R-VIPER and CP7 1 hour before stimulation with 20 nM Malp-2. Supernatants were harvested after 24 hours and assayed for IP-10 by ELISA.

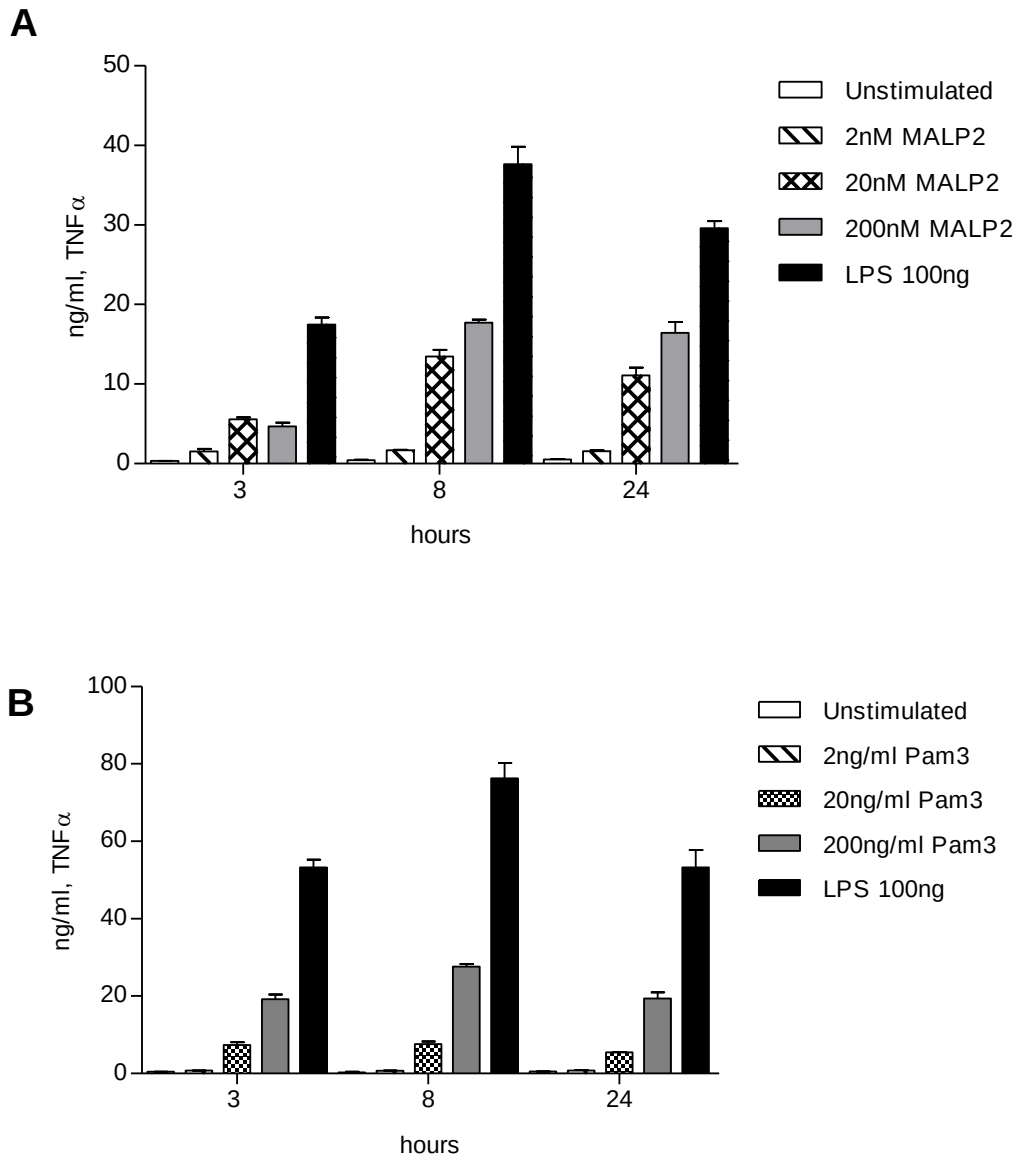

3.2.4 TLR2 and TLR4 induced dose responses for TNFα production Wt iBMDM cells were seeded at $5x10^5$ cell/ml 24hrs before treatment. Stimulation was with either, 100 ng/ml LPS, 2, 20 or 200 nM Malp-2. B. 2, 20, 200 ng/ml Pam3Csk4. After 24 hours supernatents were harvested and assayed by ELISA for TNFα.

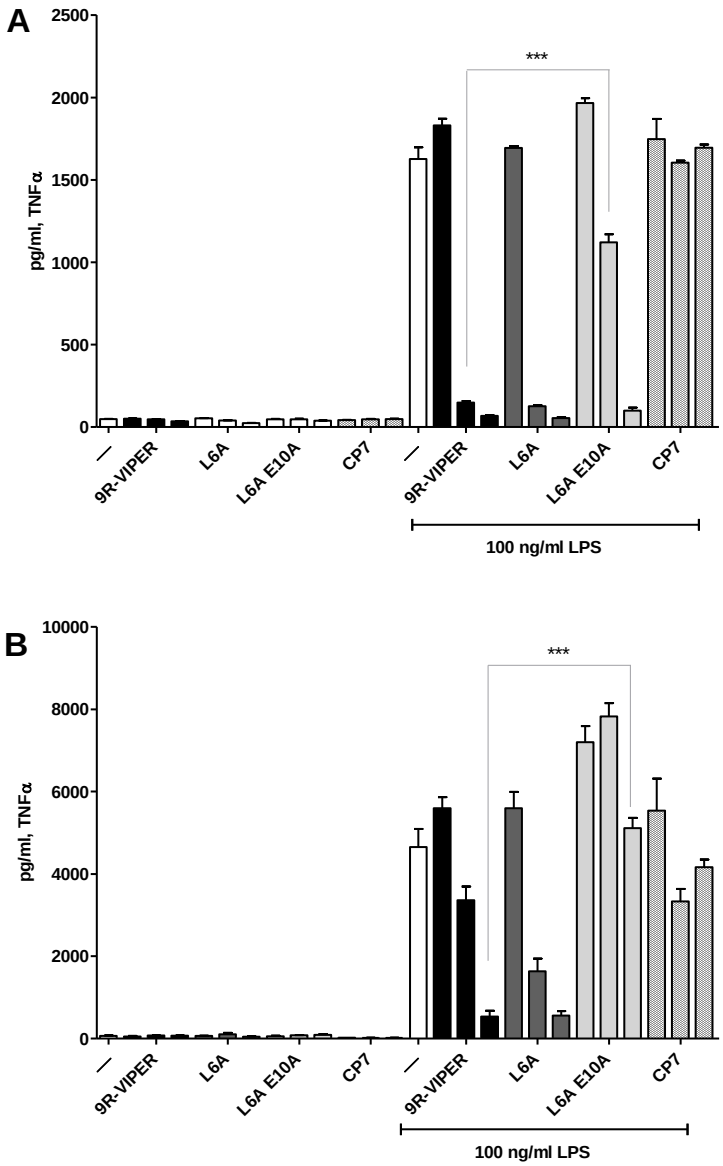

3.3.1 9R-VIPER peptide residues required for effective TLR4 signal inhibition in wt iBMDM and human PBMC. A. Wt iBMDM cells were seeded at $1x10^5$ cell/ml 24hrs before treatment. 9R-VIPER, 9R-VIPER E10A and 9R-VIPER L6AE10A, and CP7 were added at concentrations of 1, 5 and 20 μM at a volume of 2 μl 1 hour before stimulation with 100 ng/ml LPS. Supernatants were harvested after 24hrs and assayed for TNFα by ELISA. **B.** Human PBMCs were seeded at $1x10^6$ cell/ml 4 hours before treatment. Otherwise, treatments and harvesting was carried out identical to iBMDM in **A**. Supernatants were assayed for TNFα by ELISA.

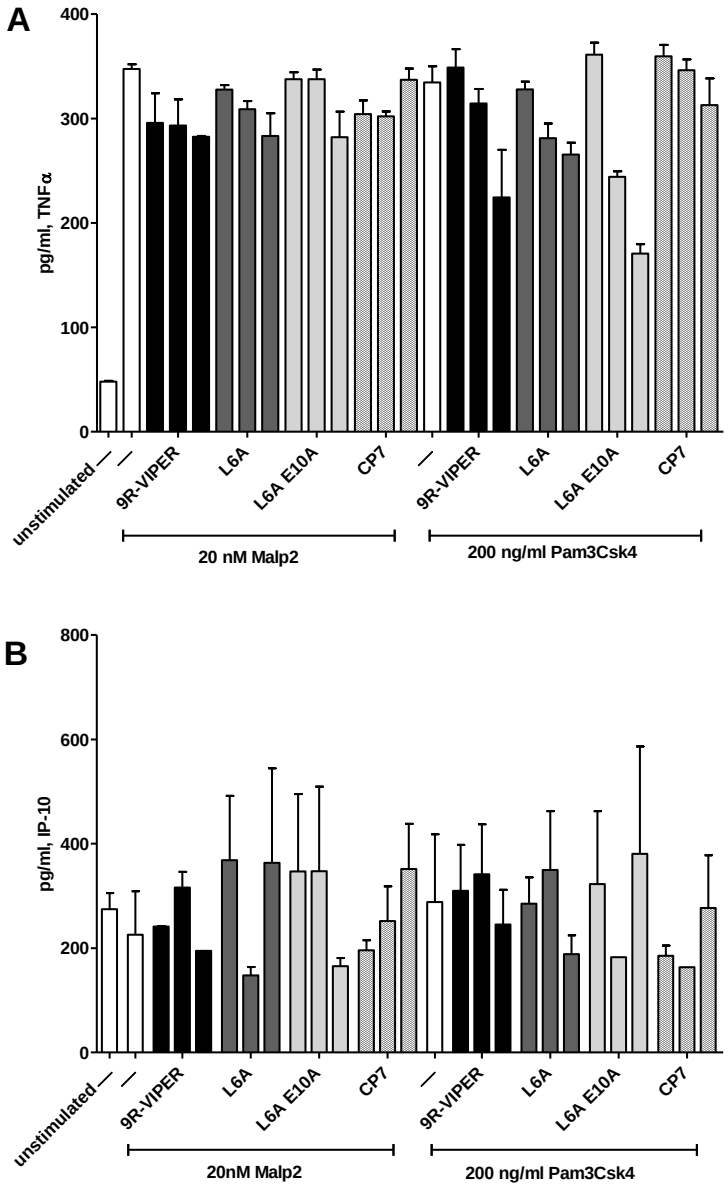

3.3.2 9R-VIPER peptide residues required for effective TLR2 signal inhibition in wt iBMDM and human PBMC A. Wt iBMDM cells were seeded at 1x105 cell/ml 24hrs before treatment. 9R-VIPER, 9R-VIPER E10A and 9R-VIPER L6AE10A, and CP7 were added at concentrations of 1, 5 and 20 μM at a volume of 2 μl 1 hour before stimulation with 20 nM Malp-2 or 200 ng/ml Pam3Csk4. Supernatants were harvested after 24hrs and assayed for TNFα by ELISA. **B.** Human PBMCs were seeded at 1x106 cell/ml 4 hours before treatment. Otherwise, treatments and harvesting was carried out identical to iBMDM in A. Supernatants were assayed for TNFα by ELISA.

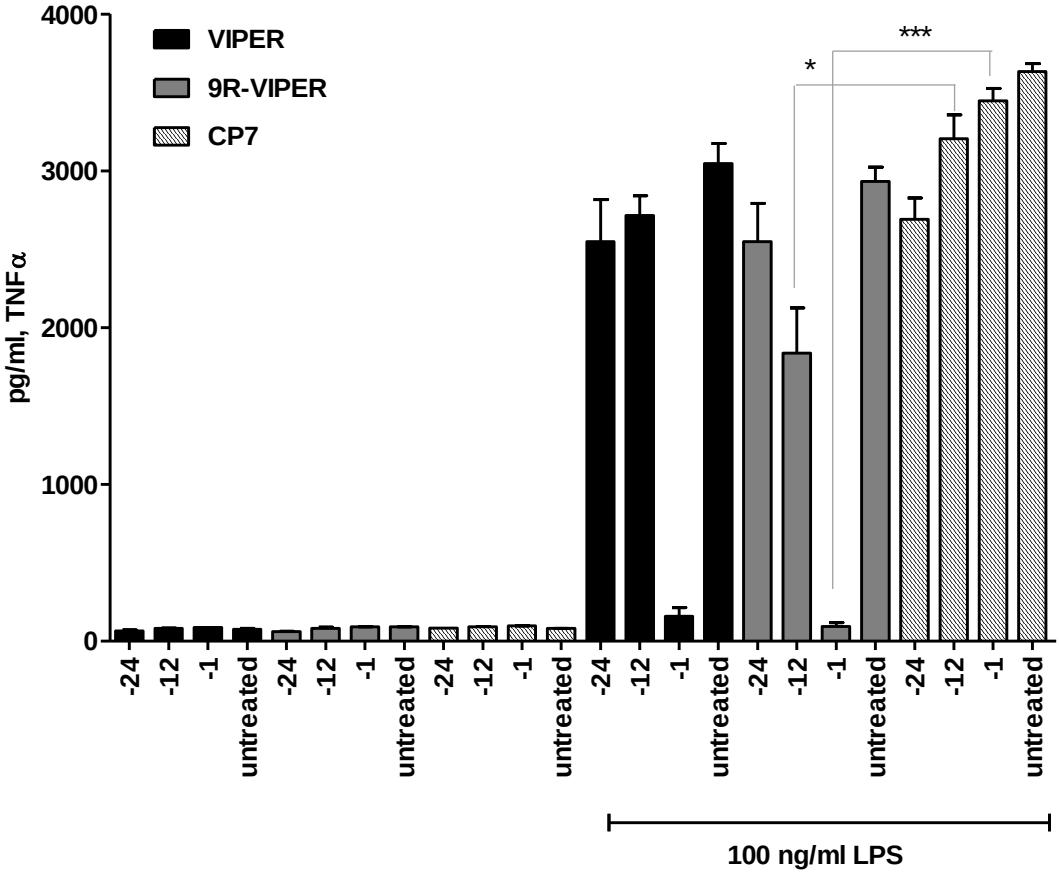

3.4.1 Longevity of TLR4 inhibition by VIPER and 9R-VIPER prior to stimulation

wt iBMDM (seeded at $1x10^5$ cells/ml) were treated with 5 μM of peptides VIPER, 9R-VIPER and CP7 at intervals of 1, 12 and 24 hours prior to 100 ng/ml LPS stimulation. Supernatants were harvested 3 hours after LPS stimulation and assayed for TNFα by ELISA.

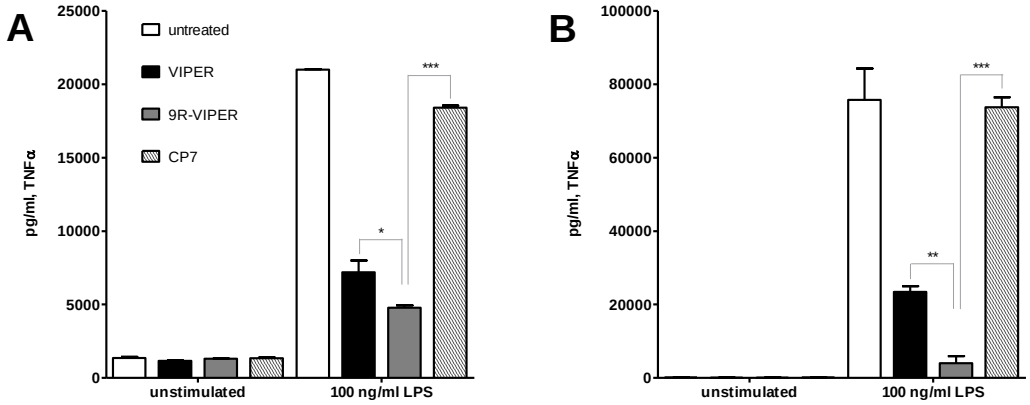

3.4.2 Longevity of TLR4 inhibition by VIPER and 9R-VIPER after stimulation. Wt iBMDM (seeded at 1x105 cells/ml) were treated with 5 μM of peptides VIPER, 9R-VIPER and CP7 1 hour prior to 100 ng/ml LPS stimulation. Supernatants were harvested (**A**) 3 and (**B**) 24 hours after LPS stimulation and assayed for TNFα by ELISA.

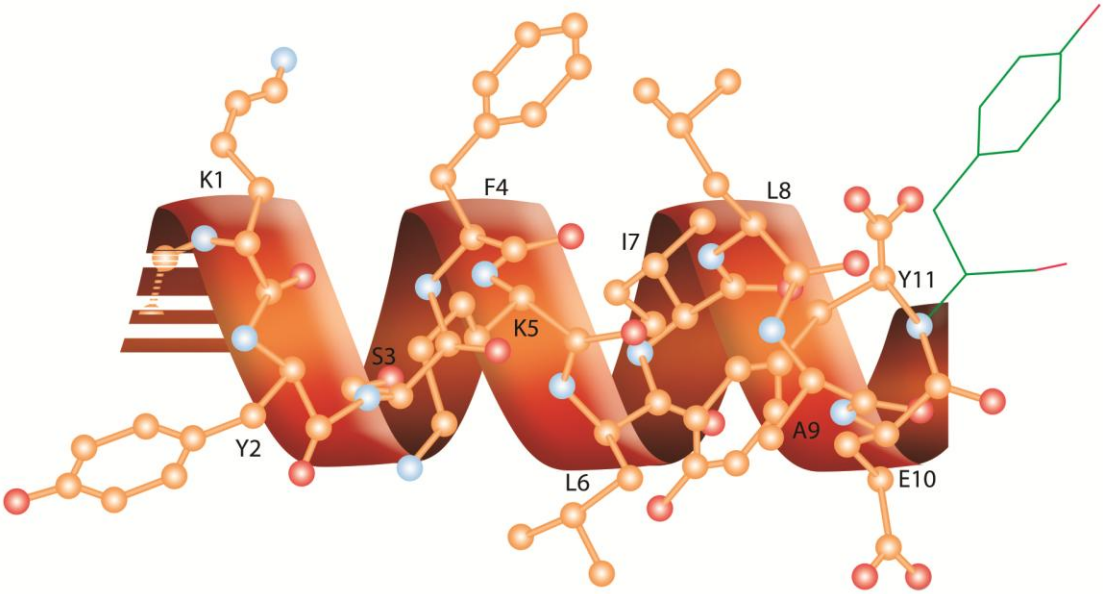

3.5.1 Cartoon representation of the 9R-VIPER 3D structure based on NRM data. Tyrosine 11 (Y11) shown in green wireframe indicates the position when VIPER motif is contained in VACV A46 according to Kim et al [79]. A significant difference was identified in the peptide version 9R-VIPER based on HN HSQC, HC HSQC, NOESY, TOCSY, and COSY investigation. The N-terminal region (left) is omitted, which contains 9 arginines in a helical confirmation. [Original Image].

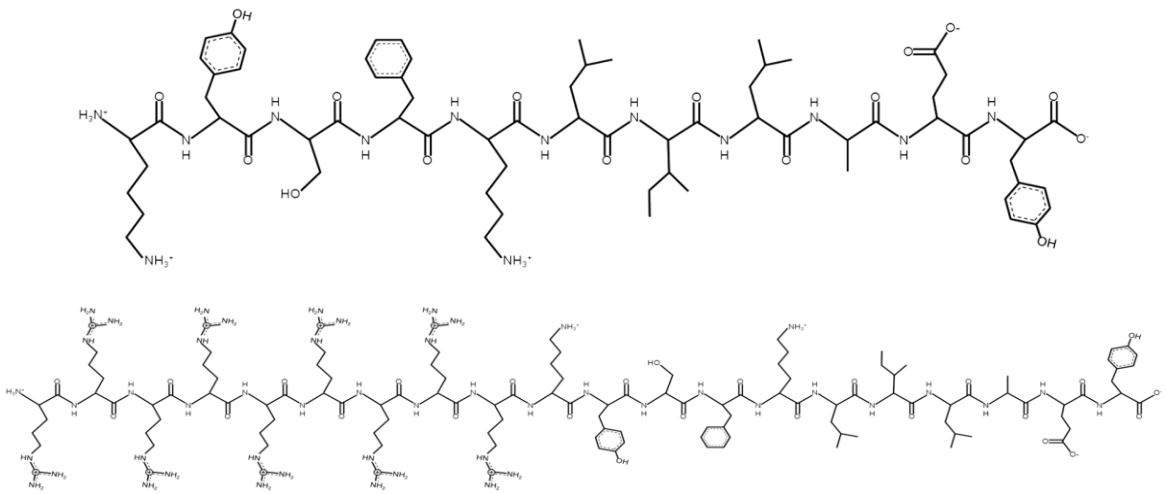

3.5.2 2D structure of VIPER and 9R-VIPER sequence

Above is pictured the 2D chemical structure of VIPER. Below is the 9R-VIPER chemical structure which contains 9 arginine residues on the N-terminus.

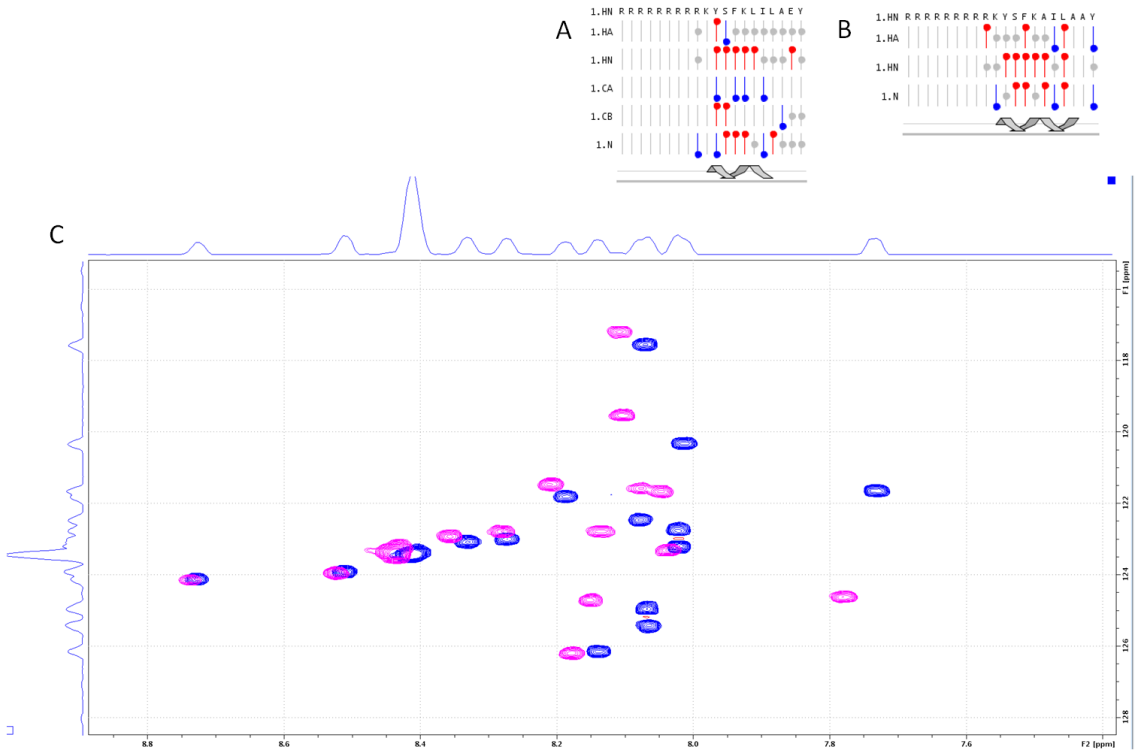

3.5.3 HN-HSQC of 9R-VIPER and 9R-VIPER L6E10A

A. 9R-VIPER shows a partial α-helical confirmation. **B.** Mutant peptide 9R-VIPER L6AE10A shows α-helical confirmation. **C.** HN-HSQC of 9R-VIPER and 9R-VIPER L6E10A overlaid in Bruker Topspin software.

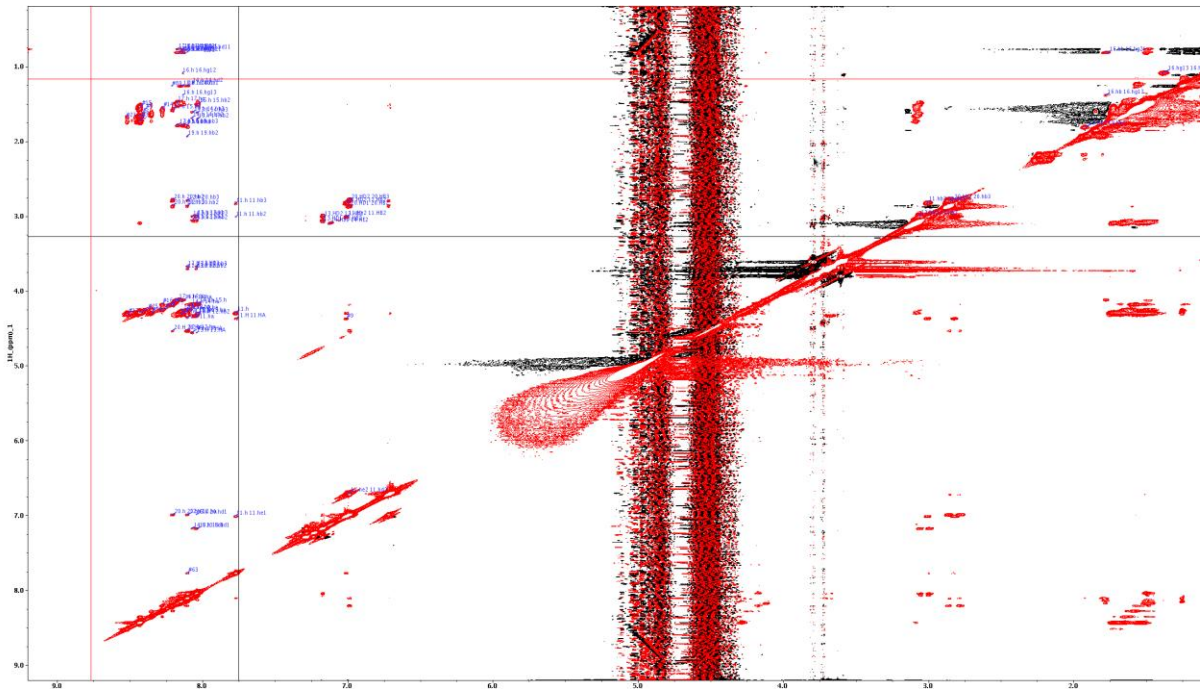

3.5.4 9R-VIPER NOESY spectrum

9R-VIPER NOESY spectrum visualised on the NMRviewJ software (OneMoon Scientific).

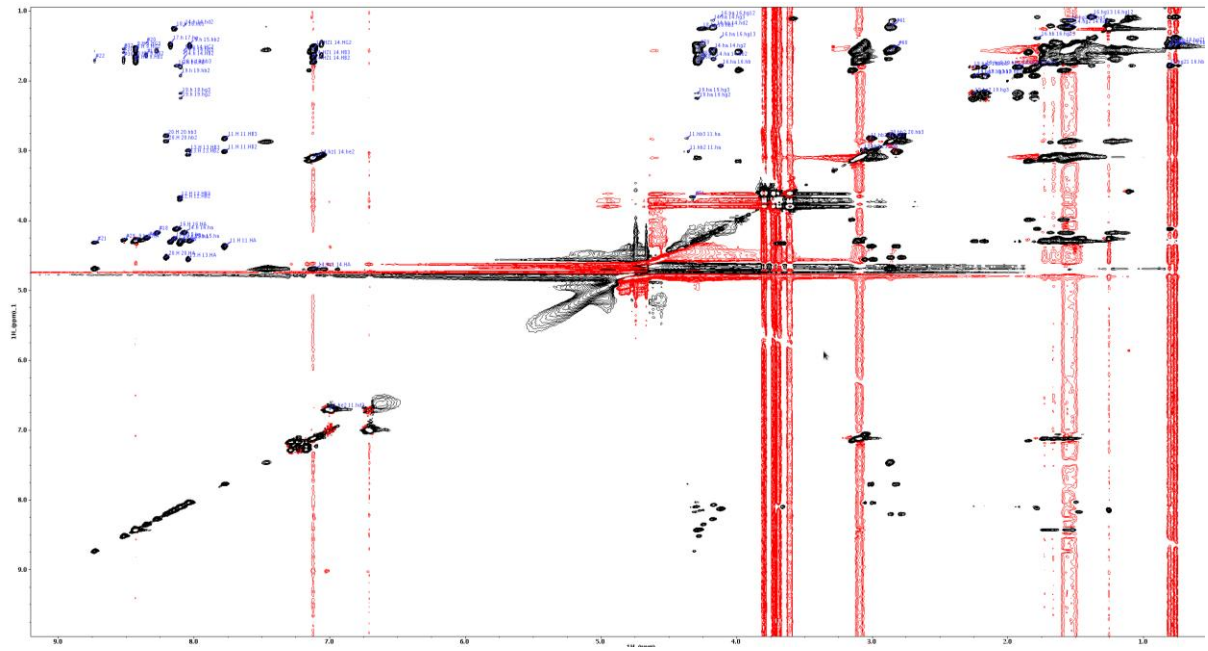

3.5.5 9R-VIPER TOCSY spectrum

9R-VIPER TOCSY spectrum visualised on the NMRviewJ software (OneMoon Scientific).

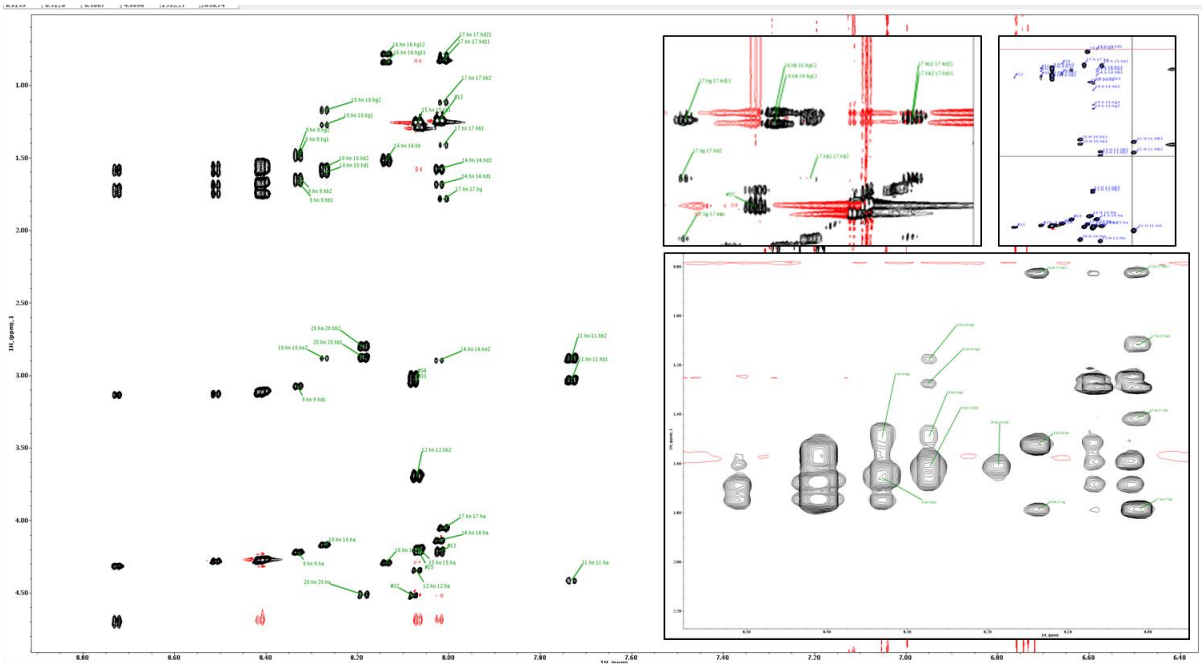

3.5.6 TOCSY/NOESY spectra sections from Mutant peptide

9R-VIPER L6E10A TOCSY/NOESY excerpt spectra visualised on the NMRviewJ software (OneMoon Scientific).

4. Discussion

The viral evasion mechanisms that are required to abate antiviral immune responses have similar results as those provided by anti-inflammatory therapeutics. Therefore, these types of viral peptides can be improved by rational design for use as therapeutics as well as providing an understanding of innate immune signalling at the molecular level. The inhibitory peptide derived from VACV A46 has been determined to retain the inhibitory properties of TLR4 pro-inflammatory signalling [46]. Currently the approach to control chronic inflammation is based on inhibition of pro-inflammatory cytokines such as TNFα and IL-1β. A more sophisticated approach is to target the upstream mechanisms of cytokine induction. Because its role in multiple inflammatory diseases, effective inhibition of the TLR4 signalling pathway is of great medical importance.

The work presented here has investigated the properties of VIPER and the affect of changing the site of the polyarginine delivery sequence. 9R-VIPER was shown to have greater inhibitory properties than VIPER for LPS driven TNFα in both wt iBMDM and primary human PBMC. This finding alone is significant in the application of 9R-VIPER as a therapeutic for pre-clinical trials in models of chronic inflammation and sepsis.

9R-VIPER was shown to be more effective than VIPER for LPS driven IFNβ in wt iBMDM and IP-10 in human PBMCs. The interferon response is classically associated as an antiviral response. Inhibition of this pathway demonstrates the evolutionary adaption that has occurred between host and poxviral pathogen. The VIPER motif of A46 allows specific inhibition of TLR4 interferon signalling, yet the full protein A46 has multiple roles in abating all TLR activity contributing to virulence [46]. The specificity of the short 11 amino acid VIPER motif presents an amiable example of the specificity of innate immune protein interactions

which is juxtaposed against the redundancy often mentioned when discussing innate immune signalling.

VIPER and 9R-VIPERwere shown to reduce TLR2-driven TNFα in wt iBMDM and human PBMC, a finding which has been investigated elsewhere but not yet produced (Stack et al. unpublished data). 9R-VIPER was shown to be slightly more effective but this difference is too slight to be determined.

When investigating the activity of 9R-VIPER for TLR2 interferon pathways the greatest challenge was identifying the subtleties in agonist dose dependencies. TLR2 also uses Mal as a signalling adaptor for signal transduction via MyD88. However, this dependency for Mal signal transduction is found to be altered by high levels of ligand stimulation [41]. The question of adaptor protein involvement for interferon induction is still under question. From the work I have carried out, it is my opinion that TLR-2 driven interferon signalling utilises differences in adaptor binding under regulation of the level of agonist encountered. The explanation of this system far surpasses the scope of any single study. This is however, an interesting topic which is sure to reveal mechanisms which are likely to be involved in other innate signalling process besides that of TLR2-driven interferon. The data presented here contributes to the earliest part of this story by confirming that either TRAM or Mal are involved in TLR-driven INFβ and IP-10 in wt iBMDM and human PBMC respectively.

The application of VIPER as an anti-inflammatory therapeutic requires a knowledge of the longevity of biological activity. Delivery of VIPER as a therapeutic agent may be provided for conditions including sepsis [64], acute pancreatitis [65, 66], acute liver failure [67, 68], ischemia/reperfusion injury [69-71], rheumatoid arthritis [72]. Therefore, the activity of

VIPER and 9R-VIPER were compared in vitro and 9R-VIPER was shown to be more effective in each aspect as regards to longevity. However, the inhibitory properties of both peptides are significantly reduced when peptide is delivered for any extended period before it is required. A characteristic such as this may be desirable for preventing instances of ischemia/reperfusion injury [69-71], leaving mild lasting effect after the required period towards other sources of inflammation such as post-surgery infection. For longer biological activity it is suggested to investigate development retro-inverso peptide inhibitors which retain bioactivity, stability, and are blood-brain barrier permeable [80]. This method employs a peptidomimetic strategy by using D-enantiomers rather than L-amino acids and reversed sequences to mimic the lead peptide conformation [81, 82]. Retro-inverso modification prolongs the half-life of peptides due to their resistance to proteosomal degradation. VIPER activity was tested when synthesised with D-enantiomers amino acids by Lysakova-Devine et al. [60] but the inverso method was not applied. This would explain the partially retained activity since binding groups are still present although confirmation would not be ideal. Retro-inversion would allow side chain binding group interactions while preventing degradation by enzymes which normally target only L-enantiomer amino acid peptides. 9R-VIPER was shown to be extremely effective at inhibiting TLR4-driven LPS for an extended period after ligand binding. This suggests that after ligand bound endocytosis, adaptor proteins are not available due to 9R-VIPER interactions.

Molecular activity of a peptide requires a specific shape and a characteristic distribution of functionalities at the binding surface. Knowledge of the possible conformational spaces of the peptide is at the core of understanding their biological activities. Because of the superior inhibitory activities of 9R-VIPER compared to VIPER this peptide was investigated using Nuclear Magnetic Resonance spectroscopy (NMR). The mutant peptide of 9R-VIPER was

shown to have lost a significant level of inhibitory activity in vitro. Because of this, the mutant peptide structure was also investigated by NMR to highlight the structural differences that occur when important amino residues are replaced.

Peptides are generally flexible structures which can adopt many rapidly interchangeable confirmations in solution. It is not feasibly possible to experimentally analyse more than a few confirmations. Protein secondary structures tend to become apparent with increasing peptide size at about 15-30 amino acids. In smaller linear peptides of 5 – 15 amino acids it is possible to see some preferred secondary structure such as helices and γ or β bends. However, these can be in rapid equilibrium with other structures and it is difficult to define a detailed structure confirmation. Understanding these mechanisms too is important for resolving immunoactivity.

In general, the different parts of each molecule has varying amounts of flexibility which can be tested by relaxation time measurements [83], NOEs [84] and coupling constants. Confirmational anylsis of a peptide requires many parameters. Solvent effects must be considered. Structure determination is assisted by collecting as many homonuclear and heteronuclear three-bond couplings as possible. Calculation of distance geometry using NOEs are standard procedure for obtaining a sampling of the confimational spaces. A difficulty in studying peptides is the large surface area to volume ratio as compared to proteins. This can promote drastic confirmation variation by interaction with solvents, receptor binding, complexation with metal ions, etc.

The assignment strategy used for 9R-VIPER and 9R-VIPER L6AE10A was sequential resonance assignment. This method involved assignment of each signal in the spectra to a

specific spin system and then assigning these spin systems to their sequential positions in the peptide chain. This method required assignment of nitrogen-proton interaction from HN-HSQC data. TOCSY was used with relatively long mixing times to give total correlations between all nuclei in each spin system. NOESY was applied to identify nuclei that were separated by less than 500ppm and is considered the most important data source for structure determination. HC-HSQC was also used to assign mostly carbon α and β in 9R-VIPER. Some difficulties were encountered in assigning long side chains with spectrum overlap, particularly in the polyarginine sequence. J-couplimgs were investigated by COSY and HMBC data was collected for assignment of carbons and protons and determination of heteronuclear long-range coupling constants, although this information has not yet been applied to the 3D structure.

Although further work may be carried out on compiling a PDB for the 3D structure of 9R-VIPER the data acquired from assignment indicates a partial α-helix confirmation. Little interaction is seen between the side chains of the VIPER sequence residue and those of the 9R delivery sequence. It is unlikely that the sequence has much affect on the biological activity in TLR4 signal inhibition besides allowing the cell membrane to be traversed efficiently. It was found, as would be expected, that the aromatic side chains of both tyrosine residues tended to show some hydrophobicity and folded back towards the backbone, sharing interactions with NH and several proton alphas. It was surprising however to find the C-terminus fold caused by the tyrosine 11 interaction with the earlier residues. Leucine 6 and glutamine acid 10 were found to share through-space interactions with their closest proton δ. The in vitro determination of L6 and E10 requirement for TLR4 signal inhibition combined with the data from NMR indicates that although linearly distant in relative terms, the L6 and E10 residues are present on the same face of the peptide helix and their long sidechains are

found in relatively close proximity. This would support the theory that these residues are important for binding of Mal and TRAM.

The NMR assignment of the mutant peptide 9R-VIPER L6AE10A was considerably easier than that of 9R-VIPER due to (i) the completed assignment of 9R-VIPER for comparison and (ii) the exceptionally clear TOCSY which was acquired with a longer mixing time of 150 ms and at a higher peptide concentration of 5mM.

The mutant peptide had alanine substitutions (with their simple short sidechain methyl group) in place of leucine 6 and glutaminc acid 10. These substitutions made the peptide sequence sidechain interactions simpler as well as easing assignment. The modifications reduced sidechain interactions and allowed for a more uniform α-helix confirmation for almost the entire peptide length (C-terminal not α-helix). The mutant peptide lost the activity of proton γ1 of tyrosine 11 side chain cross peaking with the amide proton of phenylalanine 4. The proton γ of luecine 6 was no longer present in the mutant peptide to share interactions with tyrosine 11 proton α. These differences after residue substitution caused the mutant 9R-VIPER L6AE10A to lose its inhibitory activities in vitro.

These studies are example of the effectiveness of the application of NMR for assignment and structure determination of immuno-relevant peptides. This technique has been successfully applied to both small and large molecules important for innate immune signalling [85, 86]. As discussed in the introduction of this thesis, the actual binding of both adaptor proteins Mal and TRAM has been a point of contention in the literature. A suggested step to resolving this question would be the application of NMR determination of structures of Mal and TRAM when bound to 9R-VIPER. The approach that I suggest would involve expression of

glutathione-s-transferase (GST) fusion protein of Mal and TRAM. Oda et al. have already shown expression of N-terminal His-tagged Mal [57]. His tag may be removed by cleavage with the rTEV protease. His and GST tagging would be a matter of preference so either method may be exploited. Tagged adaptor proteins could be removed and purified after VIPER peptide binding and investigated by NMR. Considerations should be given to the complex size. TIR domains of adaptor proteins should be used only and His or GST tags or any other features required for production and purification should be removed before NMR analysis.

This type of investigation would have more significant consequences than just the elucidation of a novel viral immune evasion mechanism. This study presents the findings of 9R-VIPER inhibition of signalling pathways of NFκB-dependent pro-inflammatory genes in response to TLR4 and TLR2 stimulation independently, interferon responses to both TLR4 and, more controversially, TLR2. In combination with the work presented here, the confirmation of 9R-VIPER interaction with both Mal and TRAM by NMR would confirm their involvements in these pathways, particularly interesting in respect to TLR2-driven IFNβ.

5. Conclusion

In conclusion, the work presented here confirms 9R-VIPER as more effective at TLR4 and TLR2 signal inhibition than VIPER. Novel mechanisms of TLR2-driven interferon induction have been shown to be affected by 9R-VIPER and VIPER. The longevity of TLR4 inhibition by VIPER and 9R-VIPER were determined in vitro with 9R-VIPER showing greater overall activity with room for modification to assist biological availability time. Wild type and peptides with muted residues predicted to be required for protein binding were compared and residues L6 and E10 were confirmed to be of significant importance to inhibitory activity of

9R-VIPER. The structure of 9R-VIPER and the mutant peptide L6AE10A were investigated by NMR. Important structural information was uncovered and an explanation was found for the loss of activity when important residues are changed.

This information can be used to design peptidomimetics based on 9R-VIPER and contribute to the development of a novel virally-derived TLR4 inhibitor which may ultimately have use in TLR4-dependent human disease.

6. Acknowledgements

I would like to thank my supervisor Prof Andrew Bowie for accepting me into his lab. Thank you for your kindness and the time you gave to teach and discuss our work. Thanks to Dr Kenneth Hun Mok for his helpfulness and friendliness in perusing the NMR studies.

A special thanks to Marcian Baran who has given countless time teaching and companionship in the lab. Without your help I would not have succeeded. Sincere thanks to Matteo Pennestri for teaching me the techniques required for NMR, analysis. Thanks to all the Bowie lab for their friendship during this project and to Dr Nigel Stevenson and Prof Cliona O'Farrelly for their role in this masters.

7. References

1. Xu, Y., et al., *Structural basis for signal transduction by the Toll/interleukin-1 receptor domains.* Nature, 2000. **408**(6808): p. 111-5.
2. Dunne, A., et al., *Structural complementarity of Toll/interleukin-1 receptor domains in Toll-like receptors and the adaptors Mal and MyD88.* J Biol Chem, 2003. **278**(42): p. 41443-51.
3. Nyman, T., et al., *The crystal structure of the human toll-like receptor 10 cytoplasmic domain reveals a putative signaling dimer.* J Biol Chem, 2008. **283**(18): p. 11861-5.
4. Nunez Miguel, R., et al., *A dimer of the Toll-like receptor 4 cytoplasmic domain provides a specific scaffold for the recruitment of signalling adaptor proteins.* PLoS One, 2007. **2**(8): p. e788.
5. Monie, T.P., M.C. Moncrieffe, and N.J. Gay, *Structure and regulation of cytoplasmic adapter proteins involved in innate immune signaling.* Immunol Rev, 2009. **227**(1): p. 161-75.

6. Toshchakov, V.Y. and S.N. Vogel, *Cell-penetrating TIR BB loop decoy peptides a novel class of TLR signaling inhibitors and a tool to study topology of TIR-TIR interactions.* Expert Opin Biol Ther, 2007. **7**(7): p. 1035-50.

7. Toshchakov, V.Y., et al., *Targeting TLR4 signaling by TLR4 Toll/IL-1 receptor domain-derived decoy peptides: identification of the TLR4 Toll/IL-1 receptor domain dimerization interface.* J Immunol, 2011. **186**(8): p. 4819-27.

8. Jiang, Z., et al., *Details of Toll-like receptor:adapter interaction revealed by germ-line mutagenesis.* Proc Natl Acad Sci U S A, 2006. **103**(29): p. 10961-6.

9. Gautam, J.K., et al., *Structural and functional evidence for the role of the TLR2 DD loop in TLR1/TLR2 heterodimerization and signaling.* J Biol Chem, 2006. **281**(40): p. 30132-42.

10. Medzhitov, R., et al., *MyD88 is an adaptor protein in the hToll/IL-1 receptor family signaling pathways.* Mol Cell, 1998. **2**(2): p. 253-8.

11. Fitzgerald, K.A., et al., *Mal (MyD88-adapter-like) is required for Toll-like receptor-4 signal transduction.* Nature, 2001. **413**(6851): p. 78-83.

12. Horng, T., G.M. Barton, and R. Medzhitov, *TIRAP: an adapter molecule in the Toll signaling pathway.* Nat Immunol, 2001. **2**(9): p. 835-41.

13. Yamamoto, M., et al., *Cutting edge: a novel Toll/IL-1 receptor domain-containing adapter that preferentially activates the IFN-beta promoter in the Toll-like receptor signaling.* J Immunol, 2002. **169**(12): p. 6668-72.

14. Fitzgerald, K.A., et al., *LPS-TLR4 signaling to IRF-3/7 and NF-kappaB involves the toll adapters TRAM and TRIF.* J Exp Med, 2003. **198**(7): p. 1043-55.

15. Carty, M., et al., *The human adaptor SARM negatively regulates adaptor protein TRIF-dependent Toll-like receptor signaling.* Nat Immunol, 2006. **7**(10): p. 1074-81.

16. Kagan, J.C., et al., *TRAM couples endocytosis of Toll-like receptor 4 to the induction of interferon-beta.* Nat Immunol, 2008. **9**(4): p. 361-8.

17. Valkov, E., et al., *Crystal structure of Toll-like receptor adaptor MAL/TIRAP reveals the molecular basis for signal transduction and disease protection.* Proc Natl Acad Sci U S A, 2011. **108**(36): p. 14879-84.

18. Lin, Z., et al., *Structural insights into TIR domain specificity of the bridging adaptor Mal in TLR4 signaling.* PLoS One, 2012. **7**(4): p. e34202.

19. Stack, J. and A.G. Bowie, *Poxviral protein A46 antagonizes Toll-like receptor 4 signaling by targeting BB loop motifs in Toll-IL-1 receptor adaptor proteins to disrupt receptor:adaptor interactions.* J Biol Chem, 2012. **287**(27): p. 22672-82.

20. Manavalan, B., S. Basith, and S. Choi, *Similar Structures but Different Roles - An Updated Perspective on TLR Structures.* Front Physiol, 2011. **2**: p. 41.

21. Kagan, J.C. and R. Medzhitov, *Phosphoinositide-mediated adaptor recruitment controls Toll-like receptor signaling.* Cell, 2006. **125**(5): p. 943-55.

22. Rowe, D.C., et al., *The myristoylation of TRIF-related adaptor molecule is essential for Toll-like receptor 4 signal transduction.* Proc Natl Acad Sci U S A, 2006. **103**(16): p. 6299-304.

23. Ohnishi, H., et al., *Structural basis for the multiple interactions of the MyD88 TIR domain in TLR4 signaling.* Proc Natl Acad Sci U S A, 2009. **106**(25): p. 10260-5.

24. Oshiumi, H., et al., *TIR-containing adapter molecule (TICAM)-2, a bridging adapter recruiting to toll-like receptor 4 TICAM-1 that induces interferon-beta.* J Biol Chem, 2003. **278**(50): p. 49751-62.

25. Verstak, B., et al., *The TLR signaling adaptor TRAM interacts with TRAF6 to mediate activation of the inflammatory response by TLR4.* J Leukoc Biol, 2014.

26. Gangloff, M., *Different dimerisation mode for TLR4 upon endosomal acidification?* Trends Biochem Sci, 2012. **37**(3): p. 92-8.

27. Bovijn, C., et al., *Identification of interaction sites for dimerization and adapter recruitment in Toll/interleukin-1 receptor (TIR) domain of Toll-like receptor 4.* J Biol Chem, 2012. **287**(6): p. 4088-98.

28. Ronni, T., et al., *Common interaction surfaces of the toll-like receptor 4 cytoplasmic domain stimulate multiple nuclear targets.* Mol Cell Biol, 2003. **23**(7): p. 2543-55.

29. Piao, W., S.N. Vogel, and V.Y. Toshchakov, *Inhibition of TLR4 signaling by TRAM-derived decoy peptides in vitro and in vivo.* J Immunol, 2013. **190**(5): p. 2263-72.

30. Piao, W., et al., *Recruitment of TLR adapter TRIF to TLR4 signaling complex is mediated by the second helical region of TRIF TIR domain.* Proc Natl Acad Sci U S A, 2013. **110**(47): p. 19036-41.

31. Doyle, S., et al., *IRF3 mediates a TLR3/TLR4-specific antiviral gene program.* Immunity, 2002. **17**(3): p. 251-63.

32. Hoshino, K., et al., *Differential involvement of IFN-beta in Toll-like receptor-stimulated dendritic cell activation.* Int Immunol, 2002. **14**(10): p. 1225-31.

33. Bauernfeind, F. and V. Hornung, *TLR2 joins the interferon gang.* Nat Immunol, 2009. **10**(11): p. 1139-41.

34. Dietrich, N., et al., *Murine toll-like receptor 2 activation induces type I interferon responses from endolysosomal compartments.* PLoS One, 2010. **5**(4): p. e10250.

35. Gurtler, C. and A.G. Bowie, *Innate immune detection of microbial nucleic acids.* Trends Microbiol, 2013. **21**(8): p. 413-20.

36. Kirschning, C.J. and R.R. Schumann, *TLR2: cellular sensor for microbial and endogenous molecular patterns.* Curr Top Microbiol Immunol, 2002. **270**: p. 121-44.

37. Jin, M.S., et al., *Crystal structure of the TLR1-TLR2 heterodimer induced by binding of a tri-acylated lipopeptide.* Cell, 2007. **130**(6): p. 1071-82.

38. Deininger, S., et al., *Definition of structural prerequisites for lipoteichoic acid-inducible cytokine induction by synthetic derivatives.* J Immunol, 2003. **170**(8): p. 4134-8.

39. Morath, S., et al., *Synthetic lipoteichoic acid from Staphylococcus aureus is a potent stimulus of cytokine release.* J Exp Med, 2002. **195**(12): p. 1635-40.

40. Zhu, J., et al., *Innate immunity against vaccinia virus is mediated by TLR2 and requires TLR-independent production of IFN-beta.* Blood, 2007. **109**(2): p. 619-25.

41. Kenny, E.F., et al., *MyD88 adaptor-like is not essential for TLR2 signaling and inhibits signaling by TLR3.* J Immunol, 2009. **183**(6): p. 3642-51.

42. Santos-Sierra, S., et al., *Mal connects TLR2 to PI3Kinase activation and phagocyte polarization.* Embo j, 2009. **28**(14): p. 2018-27.

43. Bowie, A.G. and L. Unterholzner, *Viral evasion and subversion of pattern-recognition receptor signalling.* Nat Rev Immunol, 2008. **8**(12): p. 911-22.

44. Smith, G.L., et al., *Vaccinia virus immune evasion: mechanisms, virulence and immunogenicity.* J Gen Virol, 2013. **94**(Pt 11): p. 2367-92.

45. Haga, I.R. and A.G. Bowie, *Evasion of innate immunity by vaccinia virus.* Parasitology, 2005. **130 Suppl**: p. S11-25.

46. Stack, J., et al., *Vaccinia virus protein A46R targets multiple Toll-like-interleukin-1 receptor adaptors and contributes to virulence.* J Exp Med, 2005. **201**(6): p. 1007-18.

47. Bowie, A., et al., *A46R and A52R from vaccinia virus are antagonists of host IL-1 and toll-like receptor signaling.* Proc Natl Acad Sci U S A, 2000. **97**(18): p. 10162-7.

48. Hutchens, M., et al., *TLR3 increases disease morbidity and mortality from vaccinia infection.* J Immunol, 2008. **180**(1): p. 483-91.

49. Hutchens, M.A., et al., *Protective effect of Toll-like receptor 4 in pulmonary vaccinia infection.* PLoS Pathog, 2008. **4**(9): p. e1000153.

50. Keating, S.E., et al., *IRAK-2 participates in multiple toll-like receptor signaling pathways to NFkappaB via activation of TRAF6 ubiquitination.* J Biol Chem, 2007. **282**(46): p. 33435-43.

51. Harte, M.T., et al., *The poxvirus protein A52R targets Toll-like receptor signaling complexes to suppress host defense.* J Exp Med, 2003. **197**(3): p. 343-51.

52. Graham, S.C., et al., *Vaccinia virus proteins A52 and B14 Share a Bcl-2-like fold but have evolved to inhibit NF-kappaB rather than apoptosis.* PLoS Pathog, 2008. **4**(8): p. e1000128.

53. Chen, R.A., et al., *Inhibition of IkappaB kinase by vaccinia virus virulence factor B14.* PLoS Pathog, 2008. **4**(2): p. e22.

54. Matta, H., et al., *Kaposi's sarcoma-associated herpesvirus (KSHV) oncoprotein K13 bypasses TRAFs and directly interacts with the IkappaB kinase complex to selectively activate NF-kappaB without JNK activation.* J Biol Chem, 2007. **282**(34): p. 24858-65.

55. Schroder, M., M. Baran, and A.G. Bowie, *Viral targeting of DEAD box protein 3 reveals its role in TBK1/IKKepsilon-mediated IRF activation.* Embo j, 2008. **27**(15): p. 2147-57.

56. Unterholzner, L., et al., *Vaccinia virus protein C6 is a virulence factor that binds TBK-1 adaptor proteins and inhibits activation of IRF3 and IRF7.* PLoS Pathog, 2011. **7**(9): p. e1002247.

57. Oda, S., E. Franklin, and A.R. Khan, *Poxvirus A46 protein binds to TIR domain-containing Mal/TIRAP via an alpha-helical sub-domain.* Mol Immunol, 2011. **48**(15-16): p. 2144-50.

58. Gonzalez, J.M. and M. Esteban, *A poxvirus Bcl-2-like gene family involved in regulation of host immune response: sequence similarity and evolutionary history.* Virol J, 2010. **7**: p. 59.

59. Shi, C.S. and J.H. Kehrl, *MyD88 and Trif target Beclin 1 to trigger autophagy in macrophages.* J Biol Chem, 2008. **283**(48): p. 33175-82.

60. Lysakova-Devine, T., et al., *Viral inhibitory peptide of TLR4, a peptide derived from vaccinia protein A46, specifically inhibits TLR4 by directly targeting MyD88 adaptor-like and TRIF-related adaptor molecule.* J Immunol, 2010. **185**(7): p. 4261-71.

61. Khor, C.C., et al., *A Mal functional variant is associated with protection against invasive pneumococcal disease, bacteremia, malaria and tuberculosis.* Nat Genet, 2007. **39**(4): p. 523-8.

62. Sheedy, F.J. and L.A. O'Neill, *The Troll in Toll: Mal and Tram as bridges for TLR2 and TLR4 signaling.* J Leukoc Biol, 2007. **82**(2): p. 196-203.

63. Toshchakov, V.Y., M.J. Fenton, and S.N. Vogel, *Cutting Edge: Differential inhibition of TLR signaling pathways by cell-permeable peptides representing BB loops of TLRs.* J Immunol, 2007. **178**(5): p. 2655-60.

64. Savva, A. and T. Roger, *Targeting Toll-Like Receptors: Promising Therapeutic Strategies for the Management of Sepsis-Associated Pathology and Infectious Diseases.* Front Immunol, 2013. **4**: p. 387.

65. Zhang, X., et al., *Possible role of toll-like receptor 4 in acute pancreatitis.* Pancreas, 2010. **39**(6): p. 819-24.

66. Xue, J. and A. Habtezion, *Carbon monoxide-based therapy ameliorates acute pancreatitis via TLR4 inhibition.* J Clin Invest, 2014. **124**(1): p. 437-47.

67. Shah, N., et al., *P59 TLR4 antagonist in acute liver failure: a novel therapeutic strategy.* Gut, 2010. **59**(Suppl 2): p. A35.

68. Shah, N., et al., *Role of toll-like receptor 4 in mediating multiorgan dysfunction in mice with acetaminophen induced acute liver failure.* Liver Transpl, 2013. **19**(7): p. 751-61.

69. Dziodzio, T., M. Biebl, and J. Pratschke, *Impact of brain death on ischemia/reperfusion injury in liver transplantation.* Curr Opin Organ Transplant, 2014. **19**(2): p. 108-14.

70. Meimei, H., et al., *Inhibiting the toll-like receptor 4 Toll/interleukin-1 receptor domain protects against hepatic warm ischemia and reperfusion injury in mice.* Crit Care Med, 2014. **42**(2): p. e123-31.

71. Lee, J.W., et al., *Renoprotective effect of paricalcitol via a modulation of the TLR4-NF-kappaB pathway in ischemia/reperfusion-induced acute kidney injury.* Biochem Biophys Res Commun, 2014. **444**(2): p. 121-7.

72. Savic, S., et al., *TLR dependent XBP-1 activation induces an autocrine loop in rheumatoid arthritis synoviocytes.* J Autoimmun, 2013.

73. Bax, A. and D.G. Davis, *MLEV-17-based two-dimensional homonuclear magnetization transfer spectroscopy.* Journal of Magnetic Resonance (1969), 1985. **65**(2): p. 355-360.

74. Liu, M., et al., *Improved WATERGATE Pulse Sequences for Solvent Suppression in NMR Spectroscopy.* Journal of Magnetic Resonance, 1998. **132**(1): p. 125-129.

75. Palmer Iii, A.G., et al., *Sensitivity improvement in proton-detected two-dimensional heteronuclear correlation NMR spectroscopy.* Journal of Magnetic Resonance (1969), 1991. **93**(1): p. 151-170.

76. Kay, L., P. Keifer, and T. Saarinen, *Pure absorption gradient enhanced heteronuclear single quantum correlation spectroscopy with improved sensitivity.* Journal of the American Chemical Society, 1992. **114**(26): p. 10663-10665.

77. Schleucher, J., et al., *A general enhancement scheme in heteronuclear multidimensional NMR employing pulsed field gradients.* Journal of Biomolecular NMR, 1994. **4**(2): p. 301-306.

78. Wishart, D.S., et al., *1H, 13C and 15N random coil NMR chemical shifts of the common amino acids. I. Investigations of nearest-neighbor effects.* Journal of Biomolecular NMR, 1995. **5**(1): p. 67-81.

79. Kim, Y., et al., *Structure of vaccinia virus A46, an inhibitor of TLR4 signaling pathway, shows the conformation of VIPER motif.* Protein Sci, 2014. **23**(7): p. 906-14.

80. Taylor, E.M., et al., *Retro-inverso prosaptide peptides retain bioactivity, are stable In vivo, and are blood-brain barrier permeable.* J Pharmacol Exp Ther, 2000. **295**(1): p. 190-4.

81. Atzori, A., et al., *Effect of sequence and stereochemistry reversal on p53 peptide mimicry.* PLoS One, 2013. **8**(7): p. e68723.

82. Fischer, P.M., *The design, synthesis and application of stereochemical and directional peptide isomers: a critical review.* Curr Protein Pept Sci, 2003. **4**(5): p. 339-56.

83. Boulat, B. and G. Bodenhausen, *Measurement of proton relaxation rates in proteins.* Journal of Biomolecular NMR, 1993. **3**(3): p. 335-348.

84. Kessler, H., et al., *Conformational dynamics detected by nuclear magnetic resonance NOE values and J coupling constants.* Journal of the American Chemical Society, 1988. **110**(11): p. 3393-3396.

85. Ablasser, A., et al., *cGAS produces a 2'-5'-linked cyclic dinucleotide second messenger that activates STING.* Nature, 2013. **498**(7454): p. 380-4.

86. Enokizono, Y., et al., *Structures and interface mapping of the TIR domain-containing adaptor molecules involved in interferon signaling.* Proc Natl Acad Sci U S A, 2013. **110**(49): p. 19908-13.

8. Abbreviations

COSY - Correlation Spectroscopy

HMBC: Heteronuclear Multiple-Bond Correlation

HMQC: Heteronuclear Multiple-Quantum Correlation

HSQC- Heteronuclear Single Quantum Correlation

HSQC: Heteronuclear Single Quantum Correlation

IRAK2 - IL-1R-associated kinase 2

IRF- Interferon regulatory factor

Mal - MyD88 adaptor-like

MAPPIT - Mammalian protein-protein interaction trap

MyD88 - Myeloid differentiation primary-response gene 88

NMR- Nuclear magnetic resonance

NOE - Nuclear Overhauser Effect

NOESY- Nuclear Overhauser Effect Spectroscopy

PAMPs - Pathogen-associated molecular patterns

PRRs - Pattern recognition receptors

SPR - Surface Plasmon resonance

Terms used - CD spectrometry - Circular dichroism spectrometry

TIR - Toll/interleukin-1 receptor homology domain

TLRs - Toll-like receptors

TOCSY - Total Correlation Spectroscopy

TRAF6 - TNFR -associated factor 6

TRAM - TRIF-related adapter molecule

TRIF - TIR domain-containing adapter inducing IFN-β

WATERGATE - Water suppression through gradient tailored excitation